The University of Alberta
Printing Department
Edmonton, Alberta

THE UNIVERSITY OF ALBERTA

SPECTROSCOPIC STUDY OF ^{32}S-NUCLEUS THROUGH THE ^{31}P(d,n) ^{32}S REACTION

by

(C) Ahmed Hassan Hussein

A THESIS

SUBMITTED TO THE FACULTY OF GRADUATE STUDIES

IN PARTIAL FULFILMENT OF THE REQUIREMENTS FOR THE DEGREE

OF MASTER OF SCIENCE

DEPARTMENT OF PHYSICS

EDMONTON, ALBERTA

FALL, 1970

UNIVERSITY OF ALBERTA

FACULTY OF GRADUATE STUDIES

The undersigned certify that they have read, and recommend to the Faculty of Graduate Studies for acceptance a thesis entitled SPECTROSCOPIC STUDY OF ^{32}S-NUCLEUS THROUGH THE ^{31}P(d,n) ^{32}S REACTION, submitted by AHMED HASSAN HUSSEIN in partial fulfilment of the requirements for the degree of Master of Science.

ABSTRACT

The $^{31}P(d,n)^{32}S$ reaction has been studied at deuteron energies of 4.0 and 5.45 MeV. Neutron energies were measured by the Time-of-Flight technique. The angular distributions of seven levels in ^{32}S-nucleus have been measured and compared with theoretical predictions of both the DWBA using the computer code DUWK and the compound statistical model using Hauser-Feshbach code. Analysis of angular distributions yields the ℓ_p values along with the absolute spectroscopic factors. The results are compared with shell model prediction and other (d,n) and (He^3,d) reactions.

ACKNOWLEDGEMENT

I would like to thank my supervisor Dr. G.C. Neilson not only for suggesting the project described in this thesis but also for his support and encouragement during the course of this work.

The efforts of Dr. J.W. McDonald in setting up the electronics and his helpful suggestions and discussions are gratefully acknowledged.

Special thanks are due to Dr. H.S. Sherif, whose invaluble and clear ideas and comments have a distinct contribution in the development of this work.

The cooperation and help of Dr. C. Glavina, Mr. S. El-Bakr and Mr. N. Mansour during the different phases of the work and the help of Messrs. A. Rashed and S. Youssef in preparing the graphs are greatly appreciated.

The excellent technical support of Messrs. J.B. Elliot, L. Holm and J.F. Easton and other members of the technical staff at the Nuclear Research Center is highly appreciated.

I am indebted to Miss Olwyn Buckland for cooperation, patience and careful typing.

I would like to thank the University of Alberta for the financial support during the period of this work.

Last but not least I would like also to thank the University of Alexandria U.A.R. for granting me a study leave.

TABLE OF CONTENTS

LIST OF TABLES

LIST OF FIGURES

CHAPTER 1

INTRODUCTION

The literature of spectroscopic studies of (d,p) and (d,n) reactions is characterized by two distinct periods of time. In the early period these reactions have been analyzed by using the Plane-Wave-Born-Approximation theories (Bu51) and (Bh52). These theories were able to predict spectroscopic quantities such as angular momenta "ℓ" of stripped particles, parities "π" of energy levels of residual nucleus, and, in some cases, a definite assignment of their spins "J". This early period came to its end with the use of the Distorted-Wave-Born-Approximation (DWBA) in calculating the angular distributions for stripping reactions. This theory is able to predict not only the above mentioned spectroscopic quantities but also in most cases it can predict correctly the magnitude of the main peak of the angular distribution. So it became easy to extract, in addition to the conventional spectroscopic quantities "ℓ, π and J", a very important quantity, 'The Spectroscopic Factor S'.

The literature of $^{31}P(d,n)\ ^{32}S$ reaction followed a track very similar to that outlined above.

Early investigations of the $^{31}P(d,n)\ ^{32}S$ reaction by Calvert et al (Ca 55) and by El-Bedewi et al. (El 55) have yielded information about the lowest energy levels in ^{32}S . Since then the only reported work on this reaction is that of Ferguson et al. (Fe 68). They carried out this reaction at $E_d = 4.9$ MeV and extracted the ℓ_p values and isobaric spins for some energy levels in ^{32}S. They did not, however, report either the

absolute magnitude of the cross-section nor spectroscopic factors.

Apart from the $^{31}P(d,n)\ ^{32}S$ reaction, the ^{32}S nucleus has been studied by other reactions. All information about ^{32}S nucleus concerned with ℓ, π, J and excitation energies below 9 MeV have been compiled by Endt et al. (En 67).

The above survey shows that the absolute magnitude of $^{31}P(d,n)\ ^{32}S$ cross-reactions and extraction of spectroscopic factors are missed from the literature. So this reaction has been done twice and ℓ, π, S, $\sigma(\theta)$ has been extracted and compared with those recently reported by Graue et al. (Gr 68) and Morrison (Mo 70) from (He^3,d) reaction at deuteron energies of 12 MeV and 15 MeV respectively. The spectroscopic factors are also compared to those obtained by Glaudmans et al. (Gl 64) from shell model calculation in the s-d shell region of nuclei.

CHAPTER 2

THEORETICAL BACKGROUND

2.1 Introduction

The study of nuclear reactions is of prime importance in the investigation of the properties of nuclear matter and of nuclei. A nuclear reaction results in general if a nucleus X , say, is bombarded with a nuclear particle a which may be a nucleus or a nucleon. Such a nuclear reaction is usually written symbolically as:

$$a + X \rightarrow Y + b \qquad 2.1$$

or, in more compact notation $X(a,b)Y$. This means that a nucleus Y has been formed by the bombardment of X with a , and the outgoing particle b carries off the excess energy originally brought in by the particle a . In the particular case that a and b are particles of the same type, Y will represent the same nucleus as X ; it will, however, be in a different quantum state from that of the bombarded nucleus (which is usually in the ground state) for all cases in which the kinetic energy of the outgoing particle differs from that of the incident particle (in the center-of-mass system).

Of course when a large number of nuclei X in a target are bombarded by a beam of particles of type a , a large number of different nuclear reactions will result. A given reaction may be studied experimentally by the detection of particles b of a specific type and having a certain particular energy; the type of particles b detected determines the nature of the nucleus Y formed in the reaction being studied, and the

energy of the outgoing particles determine the particular state Y appropriate to this reaction.

The information that can be obtained from a study of nuclear reactions may be divided into two separate categories:

1) Information concerning properties of nuclear matter in general.

2) Information concerning specific properties such as spin, parity, spectroscopic factors, etc. of the particular nuclear state Y formed in a given reaction.

As far as this work is concerned we are interested in the obtaining of information in category (2); the use of nuclear reactions as a tool for the investigation of specific properties of nuclear states, i.e., as a tool in the field of nuclear spectroscopy. For this purpose it is desirable to choose the type of nuclear reaction, or the conditions under which a given reaction is performed, so that the observations made on such reactions are directly interpretable in terms of the properties of the initial and final nuclear levels involved. If, as usual, the properties of the initial nucleus are known, the corresponding properties of the final state may then be deduced. This is not an easy job in the absence of an exact theory of nuclear reactions and lack of enough knowledge about the actual mechanisms through which the reaction of Eq. 2.1 can proceed.

Efforts in the theory of nuclear reactionsare largely devoted to attempts at finding simple models that are capable of representing one or more aspects of the experimental situation (To 61). Two models of nuclear reactions have enjoyed particular success; the compound nucleus model and the direct reaction model. According to the compound nucleus model a

nuclear reaction takes place in two steps: a) The target nucleus captures the incident particle to form a metastable state, the compound nucleus. b) The compound nucleus subsequently disintegrates to yield the reaction products. The existence of compound nucleus states of relatively long life time provides an explanation for the narrow resonances observed in nuclear cross-sections at low energies. According to the direct reaction model the transition from the incident channel to the reaction channel in a nuclear reaction takes place in one step without the formation of an intermediate state. In this model the target nucleus and incident projectile system has a life time of the order of 10^{-22} sec, assuming an interaction - potential depth of some tens of MeV. On the other hand the compound nucleus has a life time of the order of 10^{-14} sec for an energy width of the order of a fraction of an electron volt. Thus the time scales of the two mechanisms are quite different. The cross-sections predicted by the direct reaction theory do not show the sharp resonance characteristics of the compound nucleus cross-sections. A distinctive feature of the direct reaction cross-sections is the strong dependence on the direction of emission of the reaction products.

In the following we will discuss in some detail and give a quick sketch of the most successful theories for each model separately.

2.2 The Direct Reactions

The direct reaction is a one-step process. This was first recognized by Oppenheimer and Phillips (Op 35) in analyzing the low energy (d,p) reactions (La 35).

Oppenheimer and Phillips explained the reaction by noting that the deuteron is a loosely bound system (low binding energy of 2.2 MeV and radius large compared to the range of two nucleon force), and when it approaches the target nucleus the proton is detached from the deuteron due to the Coulomb field, whereas the neutron is captured. At low energies this is known as the *Oppenheimer and Phillips process*, or the *Coulomb Stripping process*, although it is now more commonly known as the *Stripping process*, at both low and high energies. In the high energy region the (d,n) and (d,p) reactions are equally probable. But what distinguishes the direct reaction from other nuclear reaction mechanisms is that the angular distribution of disintegration products is peaked in the forward direction with a very small intensity in the backward direction.

It was found that, not only the (d,n) and (d,p) reactions but also, a large number of nuclear reactions, such as (α,p) , (p,d), (n,d) , (He^3,α) , (He^3,d) and many others, showed the characteristic of *stripping* or the inverse *pick-up* reactions. Reactions of types (p,p') , (α,α') and (d,d') can also be analyzed according to the direct process.

In the use of nuclear reactions as a tool in nuclear spectroscopy one is concerned with extracting information about specific levels in the final nucleus Y . The interest of the stripping process arises from the fact that when the absorbed particle forms a definite quantum state of the residual nucleus, it must take in a certain definite orbital angular momentum and it must cause a definite change in kinetic energy. These changes in orbital angular momentum and energy are impressed on the wave functions of the outgoing particle, and a measure of the angular distribution of this particle can give a determination of ℓ - value of the absorbed particle and

hence the parity change between the initial and final states. The dependence of the angular distribution on the ℓ-value can be explained by the following simple classical arguments (Bu 57).

Consider a deuteron stripping reaction in the form

$$X^A + d \rightarrow Y^{A+1} + b \qquad 2.2$$

where $d = b+c$, d = deuteron, b = outgoing particle, c = captured particle, $Y^{A+1} = X^A + c$ = residual nucleus and X^A = target nucleus. Consider also Fig. 2-1, which represents the vector relations existing between the various particle-momenta immediately after stripping has taken place. The momentum triangle dbc shows how the original deuteron momentum $\hbar\vec{K}_d$ is shared between the outgoing and captured particle momenta, $\hbar\vec{K}_b$ and $\hbar\vec{K}_c$ respectively in the laboratory system. $\hbar\vec{q}_b$ is the internal momentum contribution to the outgoing momentum $\hbar K_b$, and vectorially we get:

$$\vec{q}_b = \vec{K}_b - \frac{1}{2}\vec{K}_d$$

$$q_b = \sqrt{K_b^2 + \frac{1}{4}K_d^2 - K_b K_d \cos\theta} \qquad 2.3$$

and

$$\vec{K}_c = \vec{K}_b - \vec{K}_d$$

$$K_c = \sqrt{K_b^2 + K_d^2 - 2K_b K_d \cos\theta} \qquad 2.4$$

The angular momentum carried by the captured particle into the target is $\hbar\vec{K}_c\eta$, where η is the classical impact parameter, for the reaction to proceed, $\hbar\vec{K}_c\eta$ must be at least as large as $\hbar\ell_c$, the orbital angular momentum of the state into which the particle c is captured, i.e.,

$$K_c\eta \geq \ell_c \qquad 2.5$$

FIGURE 2-1

Vector Relation For Deuteron Stripping

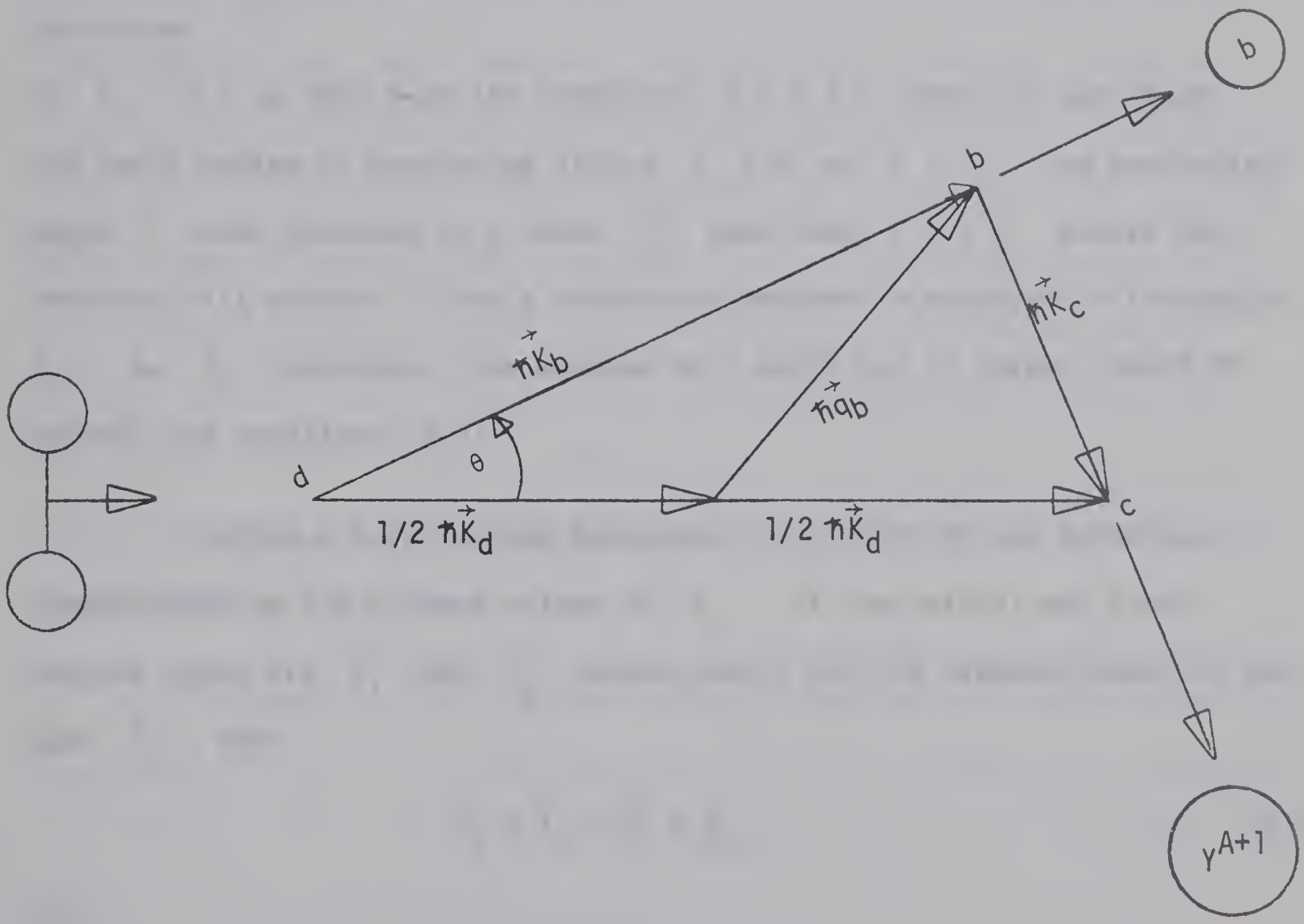
b
b
$\hbar\vec{K}_c$
$\hbar\vec{K}_b$
$\hbar\vec{q}_b$
θ
d
c
$1/2\ \hbar\vec{K}_d$
$1/2\ \hbar\vec{K}_d$
Y^{A+1}

This is a very simple expression of the conservation of angular momentum. Condition (2.5) leads to two cases of interest:

a) $\ell_c = 0$, in this case condition (2.5) will be satisfied for all values of K_c , and hence, for all angles of scattering θ . The main features determining the shape of the angular distribution will be, therefore, the fact that the deuteron will always prefer to break-up in such a way that the vector $\vec{K}_b$ is close to the direction of motion of the deuteron. In this case, $\ell_c = 0$, the angular distribution is peaked in the forward direction.

b) $\ell_c > 0$, in this case the condition $K_c \eta = \ell_c$ cannot be satisfied for small angles of scattering (since $K_c \to 0$ as $\theta \to 0$). The scattering angle θ must increase to a value θ_o such that $K_c \eta = \ell_c$ before the reaction will proceed. Thus a pronounced maximum is expected at the angle θ_o . As ℓ_c increases, this maximum will shift out to larger angles to satisfy the condition (2.5).

Taking a more quantum mechanical view point we can introduce restrictions on the allowed values of ℓ_c . If the initial and final nuclear spins are $\vec{J}_i$ and $\vec{J}_f$ respectively, and the captured particle has spin $\vec{S}_c$, then

$$\vec{J}_f = \vec{J}_i + \vec{\ell}_c + \vec{S}_c \qquad 2.6$$

i.e.

$$|J_i - J_f| - \tfrac{1}{2} \leq \ell_c \leq J_f + J_i + \tfrac{1}{2} \qquad 2.7$$

or

$$|J_i - \ell_c| - \tfrac{1}{2} \leq J_f \leq J_i + \ell_c + \tfrac{1}{2} \qquad 2.8$$

This is for the case of $S_c = \frac{1}{2}$. The parity of a quantum mechanical state with orbital angular momentum quantum number ℓ_c is $(-1)^{\ell_c}$, and hence, conservation of parity requires that

$$\pi_f = \pi_i(-1)^{\ell_c} \qquad 2.9$$

where π_i and π_f are the initial and final state parities respectively.

Additional nuclear-structure information can be obtained from the intensities of the outgoing particle groups. The deuteron stripping reactions are highly selective, strongly populating only those states in the residual nucleus that can be obtained by simply adding a neutron or a proton to the ground state of the target nucleus. Several single particle orbitals may be available for the captured particle, and the degree to which the residual nucleus satisfies this condition for a particular single particle orbital (ℓ,j) is called its *spectroscopic factor* $S(\ell,j)$ for that orbital. The $S(\ell,j)$ is unity if the state exhausts the single particle strength, as would occure in capture by a closed-shell nucleus into a pure single particle state.

A formula for the deuteron stripping angular distribution was first obtained by S.T. Butler (Bu 51) using the difficult mathematical procedure of matching,in phase and slope at the nuclear boundary, the wave functions for the external and internal regions.

Using alternative methods, several authors obtained the same or similar results to those of Butler, e.g. Bhatia et al. (Bh 52) used the Plane-Wave-Born-Approximation PWBA, and although this procedure was difficult to justify physically, later and more detailed studies (Au 53, To 54) showed

that Butler's approach was in the final analysis equivalent to the PWBA approach.

The PWBA theory was remarkably successful as a tool for identifying ℓ-values from measured angular distributions from light nuclei and even gave good fits to the shape of the main peak in the angular distribution. However,it was quickly noted (Fu 53) that the predicted absolute cross-sections were frequently too large by an order of magnitude or more. Thus, the absolute values of spectroscopic factors could not be obtained. However, the failure to predict absolute cross-sections also cast some doubt on the ability of PWBA theory to give a correct account of relative cross-sections and their dependence on energy and Q-value. As experimental data for heavier nuclei became available, where the Coulomb force at the bombarding energies usually available is too important to be ignored, it became clear that the angular distributions also deviated considerably from the expectation of the simple theory. It is now known that distortion by nuclear scattering and absorption is important, and hence, a plane-wave theory is not a good approximation.

To obtain a detailed agreement between theory and experiment for stripping reactions involving light and intermediate nuclei, and to extract spectroscopic information in the heavy-elements region, it was proposed that the interaction could be more accurately described by the distorted-wave-Born-Approximation (DWBA) (To 54). The DWBA theory takes account of the scattering and absorption of the incident deuteron before stripping, and of outgoing particle, by replacing the plane waves by distorted or elastic scattering waves. In practice, these are generated by optical-model potentials that reproduce the observed elastic scattering from the same nucleus

at the same energy, and whose parameters are therby determined. Considerable effort has gone into the exploitation of this theory, and numerous comparisons with experimental data have been done and suggested that quantitatively accurate predictions are possible (for list of references see e.g. Sa 63, Gl 63 and Le 64).

To account for the many features of the reaction, it is possible to divide it into three separate stages (El 69):

a) The projectile (deuteron) moves in the average field of the target. This field can be described by means of an optical potential, and leads to a wave function identical to the one describing the elastic scattering of deuterons.

b) A nucleon is transfered to an empty, single particle orbital in the target. In may cases, it is a good approximation to consider the target core as unchanged by this capture.

c) The outgoing particle emerges acted upon by the field of the final nucleus. This, again, is an elastic scattering problem.

These assumptions suggest that the differential cross-section can be factorized as:

$$\frac{d\sigma}{d\omega} = N\sigma_{j\ell}(\theta)\ S(\ell j) \qquad 2.10$$

$N\sigma_{j\ell}(\theta)$ is the cross-section for adding (or removing in pick-up) a particle to a pure single particle orbital (ℓ,j) , θ is the direction of the outgoing particle. The second factor $S(\ell,j)$ is the spectroscopic factor defined before, which contains the spectroscopic information. The single particle cross-section $N\sigma_{j\ell}(\theta)$ is determined by the parameters

describing the elastic scattering process.

Let us now calculate the angular distribution of the outgoing particles in the reaction $X(a,b)Y$. The Hamiltonian may be separated (Sa 65) into the Hamiltonian of the colliding pair when not interacting (well separated),and the interaction V between them,

$$H = H_\alpha + V_\alpha + T_\alpha \qquad 2.11$$

$$= H_\beta + V_\beta + T_\beta \qquad 2.12$$

where $H_\alpha = H_X + H_a$ and T_α is the kinetic energy operator of the colliding pair X and a . The total wave function of the system satisfies the Schrodinger equation

$$(E-H)\Psi = 0 \qquad 2.13$$

while the wave functions of the internal states of the pair are given by

$$(E_\alpha - H_\alpha)\psi_\alpha = 0 \ , \ (E_\beta - H_\beta)\psi_\beta = 0$$

$$\psi_\alpha = \psi_X \psi_a \qquad 2.14$$

and $E_\alpha = E_X + E_a$, and the total energy of the system is given by:

$$E = E_\alpha + \hbar^2 k_\alpha^2 \ / \ 2m_\alpha$$
$$= E_\beta + \hbar^2 k_\beta^2 \ / \ 2m_\beta \qquad 2.15$$

where k_α is the wave number of the relative motion of the X and a and m_α is their reduced mass.

The theory of direct nuclear reactions is concerned with calculating the transition amplitudes for various types of nuclear reactions on

the basis outlined above. The direct interactions can be treated as a perturbation (To 61), the transition amplitude is then given by the matrix element

$$T_{\alpha\beta}(\vec{k}_\alpha, \vec{k}_\beta) = \langle \Psi_\beta^{(-)}(\vec{k}_\beta) | V_\beta - U_\beta | \Psi_\alpha^{(+)}(\vec{k}_\alpha) \rangle \qquad 2.16$$

where the α and β subscripts represent the entrance and exit channels respectively. The plus (minus) superscript denotes that, asymptotically, the incoming (outgoing) part of the wave function Ψ becomes identical with the incoming (outgoing) part of a plane wave. V_β is the interaction potential between the two nuclei in the exit channel, and U_β is the optical potential in the exit channel.

The DWBA follows from the observation that the elastic scattering is usually the dominant process. This is unambiguous in the asymptotic region, but we need the wave function over all space and particularly in the interior region where the projectile and the target are strongly interacting. The usual procedure is to obtain the optical potential which reproduces the observed elastic scattering of a on X , and which thus reproduces the asymptotic wave function accurately. It is then assumed that this same optical model wave-functions may be extrapolated into the interior region of strong interaction where a and X approach closely. That is we use (Sa 65)

$$\Psi_\alpha^{(+)} \simeq \psi_\alpha \chi_\alpha^{(+)}(k_\alpha) \qquad 2.17$$

and the matrix element (2.16) becomes:

$$T_{\alpha\beta}(\vec{k}_\alpha, \vec{k}_\beta) = \langle \psi_\beta \chi_\beta^{(-)} | V_\beta - U_\beta | \psi_\alpha \chi_\alpha^{(+)} \rangle \qquad 2.18$$

where χ's are the eigenfunctions of the corresponding optical potential, i.e.

$$\{\nabla^2+k^2 - \frac{2\mu}{\hbar^2}[U(r)+U_c(r)]\}\chi(\vec{k},\vec{r}) = 0 \qquad 2.19$$

where $U_c(r)$ is the Coulomb potential.

Since the incident particle $a = b+c$ where b is the outgoing particle and c is the captured particle, then we also have $Y = X+c$ so the interaction potential $V_\beta - U_\beta$ becomes:

$$V_\beta - U_\beta = V_{bY} - U_{bY} = V_{bc} + (V_{bX} - U_{bX}) \qquad 2.20$$

it is customary to take V_{bc} as the important interaction term for many reasons (Sa 65, G1 63, E1 69).

Consider a (d,n) reaction then Eqn. 2.18 can be rewritten as

$$T = \int d\vec{r}_d \int d\vec{r}_n \chi_n^{*(-)}(\vec{k}_n,\vec{r}_n)\langle Y,n|V_{np}|X,d\rangle \chi_d^{+}(\vec{k}_d,\vec{r}_d) \qquad 2.21$$

The central factor is the matrix element of the interaction V_{np} taken between the internal states of the colliding pairs,

$$\langle Y,n|V_{np}|X,d\rangle = \int d\eta \psi_y^* \psi_n^* V_{np} \psi_X \psi_d \qquad 2.22$$

it implies integration over all internal coordinates η independent of $\vec{r}_d$ and $\vec{r}_n$, where $\vec{r}_d$ is the separation of the centers of mass of X and d and $\vec{r}_n$ is that of Y and n. This matrix element then remains a function of $\vec{r}_d$ and $\vec{r}_n$. It plays the role of an effective interaction or form factor for the transition between the elastic scattering states $\chi_\alpha^{(+)}$ and $\chi_\beta^{(-)}$. It contains all the information on nuclear structure, angular momentum selection rules, and even the type of reaction being considered (stripping, inelastic scattering, knock-on, etc.). This factorization

of the integrand of the amplitude 2.21 has the practical advantage that one computer program can treat a whole variety of nuclear models and reaction modes. All we need is a number of optional subroutines to calculate the relevant form factors.

We can now write the nuclear matrix element 2.22 as

$$\langle y,n|V_{np}|X,d\rangle = \langle J_y M_y, S_n m_n|V_{np}|J_X M_X, S_d m_d\rangle$$

$$= \int \psi^*_{J_y M_y}(\eta_X \eta_p, \vec{r}_{pX}) \psi^*_{S_n m_n}(\eta_n)$$

$$V_{np}(r_{np})\ \psi_{S_d m_d}(\eta_n \eta_p, r_{np}) \psi_{J_X M_X}(\eta_X) d\eta_n d\eta_p\ d\eta_X \qquad 2.23$$

In writing Eqn. (2.23) we assumed that the potential V_{np} is a central potential, and the residual necleus Y is formed by just adding a proton to an inert core (target nucleus). The η_i represents the internal coordinates of particle i while the r_{ij} represents the vector joining the centers of mass of i and j . The above assumptions will enable us to expand $\psi^*_{J_y M_y}(\eta_X \eta_p, \vec{r}_{px})$ as

$$\psi^*_{J_y M_y}(\eta_X \eta_p, \vec{r}_{px}) = \sum_j \langle JjM\mu | J_y M_y\rangle \psi^*_{JM}(\eta_X) \phi^*_{j\mu}(\eta_p, \vec{r}_p) \qquad 2.24$$

where $\phi_{j\mu}$ may be called the captured proton wave function, and $\langle JjM\mu | J_y M_y\rangle$ is the Clebsch-Gordan coefficient as defined by Rose (Ro 61). η_p now refers to the proton spin coordinate. $\phi_{j\mu}$ can be expanded further as,

$$\phi_{j\mu}(\eta_p, \vec{r}_p) = \sum_{\ell m} \langle \ell \tfrac{1}{2}\ m\ \mu-m | j\mu\rangle R_{\ell j}(r_p)\ i^{\ell} Y^m_{\ell}(\theta_p, \phi_p) \psi_{\frac{1}{2}\mu-m}(\eta_p) \qquad 2.25$$

because the parity is $(-)^{\ell}$ only those ℓ-values satisfying Eqn. 2.9 are

allowed. It is customary to regard $\phi_{j\mu}$ as proportional to the shell model single particle wave function for the orbital $(n\ell j)$ (Sa 65) so that,

$$R_{\ell j}(r) = \sqrt{S_{\ell j}}\, u_{n\ell j}(r) \qquad 2.26$$

where $u_{n\ell j}(r)$ is the normalized radial wave function and $S_{\ell j}$ is the usual spectroscopic factor.

The internal deuteron wave function appears in Eqn. 2.23 can be written as, (neglecting the D-state of the deuteron)

$$\psi_{S_d m_d}(\eta_n \eta_p, r_{np}) = \psi_{1 m_d}(\eta_n \eta_p, r_{np})$$

$$= \phi_d(r_{np}) \sum_{m'_n} \left\langle \tfrac{1}{2}\, \tfrac{1}{2}\, m'_n m_d - m'_n \middle| 1 m_d \right\rangle$$

$$\psi_{\frac{1}{2} m'_n}(\eta_n)\, \psi_{\frac{1}{2} m_d - m'_n}(\eta_p) \qquad 2.27$$

Now substituting Eqn. (2.2_4) in the nuclear matrix element (2.23) we get,

$$\left\langle J_y M_y, \tfrac{1}{2} m_n \middle| V_{np} \middle| J_X M_X, 1 m_d \right\rangle = \sum_j \langle Jj M\mu | JyMy \rangle$$

$$\int \phi^*_{j\mu}(\eta_p, \vec{r}_p) \psi^*_{\frac{1}{2} m_n}(\eta_n) V_{np}(r_{np})\ \ \psi_{1 m_d}(\eta_n \eta_p, r_{np})$$

$$d\eta_n d\eta_p \int \psi^*_{JM}(\eta_X) \psi_{J_X M_X}(\eta_X) d\eta_X \qquad 2.28$$

carrying out the integration over η_X we get,

$$\left\langle J_y M_y, \tfrac{1}{2} m_n \middle| V_{np} \middle| J_X M_X, 1 m_d \right\rangle = \sum_{\ell j} \langle J_X j M_X \mu | J_y M_y \rangle \int \phi^*_{j\mu}(\eta_p, \vec{r}_p) \psi^*_{\frac{1}{2} m_n}(\eta_n)$$

$$V_{np}(r_{np})\ \ \psi_{1 m_d}(\eta_n \eta_p, r_{np}) d\eta_n d\eta_p \qquad 2.29$$

Substituting Eqns. (2.25) and (2.27) in (2.29) we get,

$$\langle J_y M_y, \tfrac{1}{2} m_n | V_{np} | J_X M_X, 1 m_d \rangle =$$

$$\sum_{\ell j m m'_n} \langle J_X j M_X \mu | J_y M_y \rangle \langle \ell \tfrac{1}{2} m \ \mu-m | j\mu \rangle \langle \tfrac{1}{2} \tfrac{1}{2} m'_n m_d - m'_n | 1 m_d \rangle$$

$$R_{\ell j}(r_p) [i^{\ell} Y^{m}_{\ell}(\theta_p, \phi_p)]^{*} V_{np}(r_{np}) \phi_d(r_{np})$$

$$\int\int \psi^{*}_{\frac{1}{2}\, \mu-m}(\eta_p) \psi^{*}_{\frac{1}{2}\, m_n}(\eta_n) \ \psi_{\frac{1}{2}\, m'_n}(\eta_n) \ \psi_{\frac{1}{2}\, m_d - m_n}(\eta_p)$$

$$d\eta_n d\eta_p$$

carrying out the integrations over η_n and η_p the nuclear matrix element reduces to,

$$\langle J_y M_y, \tfrac{1}{2} m_n | V_{np} | J_X M_X, 1 m_d \rangle =$$

$$\sum_{\ell j m} \langle J_X j M_X \mu | J_y M_y \rangle \langle \ell \tfrac{1}{2} m \ \mu-m | j\mu \rangle \langle \tfrac{1}{2} \tfrac{1}{2} m_n m_d - m_n | 1 m_d \rangle$$

$$R_{\ell j}(r_p) [i^{\ell} Y^{m}_{\ell}(\theta_p, \phi_p)]^{*} D(r_{np}) \qquad 2.30$$

where $$m = \mu + m_n - m_d \qquad 2.31$$

and $$D(r_{np}) = V_{np}(r_{np}) \ \phi_d(r_{np}) \qquad 2.32$$

Another approximation, concerning the potential V_{np}, can be done here, namely, the zero range approximation, which consists of putting,

$$D(r_{np}) = D_o \ \delta(r_{np}) \qquad 2.33$$

Now the deuteron wave function should satisfy the Schrodinger equation,

$$(\nabla^2 - \alpha^2)\,\phi_d(s) = (M/\hbar^2)D(s) \qquad 2.34$$

and the constant D_o in Eqn. (2.33) may be chosen to give the correct volume integral over D .

$$D_o = \int D(s)\,\vec{ds} \qquad 2.35$$

$$= \frac{\hbar^2}{M}\int(\nabla^2 - \alpha^2)\phi_d(s)\,\vec{ds}$$

$$= -\frac{\alpha^2\hbar^2}{M}\int\phi_d(s)\,\vec{ds}$$

$$= -\varepsilon\int\phi_d(s)\,\vec{ds} \qquad 2.36$$

where $\varepsilon = \alpha^2\hbar^2/M$ is the binding energy of the deuteron.

The deuteron wave function $\phi_d(s)$ can be taken as the Hulthen wave function.

$$\phi_d(s) = \frac{\alpha\beta(\alpha+\beta)}{2\pi(\alpha-\beta)^2}\cdot\frac{e^{-\alpha s} - e^{-\beta s}}{s} \qquad 2.37$$

Substituting this in Eqn. 2.36 we get,

$$D_o^2 \simeq 1.65 \times 10^4 \quad \mathrm{MeV}^2\cdot\mathrm{F}^3 \qquad 2.38$$

The matrix element of Eqn. (2.21), now becomes:

$$T = \sum_{\ell jm}\sqrt{s_{\ell j}}\;D_o\;\langle J_X j M_X \mu \,|\, J_y M_y\rangle$$

$$\langle \ell\;\tfrac{1}{2}\;m\;\mu-m\,|\,j\mu\rangle\langle\;\tfrac{1}{2}\;\tfrac{1}{2}\;m_n\;m_d-m_n\,|\,1m_d\rangle$$

$$\int d\vec{r}\;\chi^{*(-)}(\vec{k}_n,\vec{r})\;u^*_{n\ell j}(r)\;[i^{\ell}Y^m_{\ell}(\theta,\phi)]^*$$

$$\chi^{(+)}(\vec{k}_d,\vec{r})\;. \qquad 2.39$$

The differential scattering cross-section is then given by

$$\frac{d\sigma}{d\Omega} = \frac{\mu_\alpha \mu_\beta}{(2\pi\hbar^2)^2} \frac{k_n}{k_d} \frac{\sum_{M_X M_y m_n m_d} |T|^2}{(2J_X+1)(2S_d+1)} \qquad 2.40$$

The procedure of computing the transition matrix element of Eqn. 2.21 can be summarized as follows:

1) The nuclear matrix element is well defined except for the shell model radial wave function $u_{n\ell j}(r)$. This is a bound state wave function for the captured particle. This wave function satisfies two Shrodinger equations; the first contains the nuclear potential for the internal region, and the second,for the asymptotic region,contains only the coulomb potential. The first equation is solved with a Woods-Saxon nuclear potential form with a trial depth and this solution is matched to the solution of the asymptotic region. If the matching process gives the correct binding energy of the captured particle with the target nucleus, then we get the correct radial wave function. On the other hand, if the matching process gives the wrong binding energy. The depth of the nuclear potential should be changed and the whole process is repeated until we get the correct binding energy.

Once we get the correct radial wave function of the captured proton the nuclear matrix element of Eqn. 2.39 is completely defined.

2) In order to get the distorted wave for both the incident deuteron and outgoing neutron, the corresponding Schrodinger equation of the form given in Eqn. 2.19 should be solved. This requires a knowledge of the appropriate optical potential parameters. These are usually fixed by fitting the elastic

scattering data of the projectile-target system at the same incident energy and likewise the outgoing particle-residual nucleus system.

Once the optical potentials are defined, we can proceed to the next step, namely, solving the distorted waves' Schrodinger equation.

3) To solve the Schrodinger equations for the distorted waves, we use the usual partial wave expansion (Sa 64a), and the solution in case of a charged particle is matched asymptotically to

$$\chi_{LJ}(k,r) = \frac{i}{2} [H_L^*(k,r) - \eta_{LJ} H_L(k,r)] \exp(i\rho_L) \qquad 2.41$$

where ρ_L is the Coulomb phase shift. Eqn. 2.41 represents the solution at large r beyond the range of nuclear potential where,

$$H_L(k,r) = G_L + iF_L \qquad 2.42$$

is the outgoing Coulomb wave function and η_{LJ} is the reflection coefficient for the (L,J) wave, which can be obtained from the matching process.

For neutral particles the asymptotic solution is the outgoing and ingoing spherical waves.

4) Now after doing steps 1,2, and 3 above the transition matrix element T can be computed, and so is the angular distribution of Eqn. 2.40.

The above treatment is the most simple treatment for computing the angular distribution of $a(d,n)$ reaction. Additional refinements of the model have appeared in the literature, e.g.

1) Use of finite range potential instead of the δ-function potential of Eqn. (2.33),

2) Use of different forms of the optical potential such as adding a spin orbit term and/or surface or volume for the real and imaginary parts,

3) Inclusion of the d-state of the deuteron, and

4) Use of non-local potentials.

2.3 Compound Nucleus Reactions

As mentioned before (Sec. 2.1) the compound nucleus model divides the nuclear reaction into two steps. The first step is the union of the colliding pair into a single unit, the so called *compound nucleus*. This compound nucleus, although not stable, has many of the properties of stable nuclei. In particular, it has rather well-defined energy levels. The second part of the reaction is the disintegration of the compound nucleus, either into the pair from which it was formed or into another pair. This disintegration is subject to probability laws, once the compound nucleus has been formed the probability of a particular mode of disintegration is independent of the mode of formation.

The probability of the formation of a compound nucleus is small unless the energy of the colliding pair coincides very closely with one of the energy levels of the compound nucleus. On the other hand, if the coincidence is perfect, the cross-section for the formation of the compound nucleus shows, as a function of the incident energy, sharp maxima but drops to small values in between. These sharp maxima (called resonances) are ususally narrow and closely spaced. These resonances are individually of interest only at low energies. At higher energies, with increasing numbers of resonances, the physical interest (and usually the measurements itself) concerns nuclear cross-sections averaged over the resonances. The statistical theory of nuclear

reactions deals with such average cross-sections.

The treatment of average cross-sections employs an evaporation model. The evaporation model assumes that the compound nucleus, in its decay, loses all memory of the way in which it was formed, and treats all possible decay products as equally probable.

In the following we will follow an article by Vogt (Vo 68).

The evaporation model was first proposed by Bethe and Weisskopf, in this model a nuclear reaction was of the following kind:

Initial projectile and target nucleus (labelled c) → compound nucleus → reaction products (labelled c') is assumed to have an average cross-section $\bar{\sigma}_{cc'}$, which may be factored,

$$\bar{\sigma}_{cc'} = [\sigma_{comp}(c)][\frac{G_{c'}}{G}] \quad . \qquad 2.42$$

The average of the cross-section is over any resonance structure. The first factor on the r.h.s. of Eqn. (2.42) depends only on the initial pair of particles c , and is called a cross-section for the formation of the compound nucleus, the second factor depends only on the final reaction products c' and is called the branching ratio. The denominator of the branching ratio is a sum of the factor $G_{c'}$ over all reaction products (including c and c') available to the compound nucleus,

$$G \equiv \sum_{c''} G_{c''} \qquad 2.43$$

The factorization assumed in Eqn. (2.42) is an expression of the independence of formation and decay of the compound nucleus.

Using the receiprocity theorem Eqn. 2.42 can be written as

$$\overline{\sigma}_{cc'} = \sigma_{comp}(c) \frac{k^2_{c'} \sigma_{comp}(c')}{\sum_{c''} k^2_{c''} \sigma_{comp}(c'')} \qquad 2.44$$

where k_c is the wave number for the relative motion of the pair c. The evaluation of the denominator of Eqn. 2.44 requires an enumeration of all the possible reaction products. To carry out the enumeration, we describe each reaction alternative or channel c (Bl 52) by the following set of quantum numbers,

$$c \equiv (\alpha, I, i, s, \ell, J, M_J, \pi) \qquad 2.45$$

where α labels the pair of particles in the channel c represented by "p" and their state of excitation E^*_p where

$$E^*_p = E_p^{max} - E_p \qquad 2.46$$

$$E_p^{max} = E + Q \qquad 2.47$$

where E is the C.M. energy of the initial pair, E_p is the center of mass energy of the pair p, and Q is the Q-value of the reaction. I and i are the intrinsic spins of the pair of particles α, s is the channel spin,

$$\vec{s} = \vec{I} + \vec{i} \qquad 2.48$$

ℓ is the orbital angular momentum of the pair, J is the total angular momentum,

$$\vec{J} = \vec{\ell} + \vec{s} = \vec{\ell} + \vec{I} + \vec{i} = \vec{J} + \vec{I} \qquad 2.49$$

M_J is the z-component of J, and π is the total parity. The average cross-section $\overline{\sigma}_{\alpha\alpha'}$, can now be written as,

$$\overline{\sigma}_{\alpha\alpha'} = \frac{\pi}{k_\alpha^2} \sum_{J,\pi} \frac{(2J+1)}{(2I+1)(2i+1)} \{\sum_{s\ell} T_\ell(\alpha)\}$$

$$\{\frac{\sum_{s'\ell'} T_{\ell'}(\alpha')}{\sum_{\alpha''s''\ell''} T_{\ell''}(\alpha'')}\} \qquad 2.49$$

The unprimed quantities refer to the incoming channels of the reaction, the primed quantities refer to the outgoing channels, and double primed quantities in the denominator are summed over all channels to which the compound nucleus can decay. $T_\ell(\alpha)$ are called *transmission functions* and are given by the optical model phase shifts $\delta_{\alpha\ell}$ of the pair α,

$$T_\ell(\alpha) \equiv 1 - \left|e^{2i\delta_{\alpha\ell}}\right|^2 \qquad 2.50$$

Those transmission functions are independent of J and s if the optical model potential does not contain spin-dependent terms, otherwise they should be included i.e., we replace each $\sum_{s\ell} T_\ell(\alpha)$ by $\sum_{j\ell} T_{\ell j}(\alpha)$, where

$$T_{\ell j} \equiv 1 - \left|e^{2i\delta_{\ell j\alpha}}\right|^2 \qquad 2.51$$

we can now define a channel wave function ψ_c, describing all the properties of the channel except the radial motion,

$$\psi_c = r_c^{-1} \Phi_\alpha \sum_{m_\ell m_s} \langle \ell s m_\ell m_s | J m_J \rangle \; Y_{\ell m_\ell} X_{s m_s} \qquad 2.52$$

where r_c is relative separation of the pair of particles in each channel, Φ_α is the state of internal motion of the two particles in the channel, X_{sm_s} is the wave function of the coupled intrinsic-spins I

and i of the two particles.

Outside the compound nucleus the whole wave function of the system can be written as

$$\Psi = \sum_c \phi_c \psi_c \qquad 2.53$$

where ϕ_c is the radial wave function in channel c , outside the nuclear potential the radial wave equation is

$$\frac{d^2\phi_c}{dr_c^2} - \frac{\ell(\ell+1)}{r_c^2}\phi_c - \frac{2\eta_c k_c}{r_c}\phi_c + k_c^2\phi_c = 0 \qquad 2.54$$

where $\eta_c (\equiv Z_1 Z_2 e^2/\hbar v_c)$ is the Coulomb parameter. The regular and irregular solutions of Equation 2.45 are F_c and G_c respectively which are normalized by their Wronskian,

$$G_c \frac{dF_c}{dr_c} - F_c \frac{dG_c}{dr_c} = k_c \qquad 2.55$$

The outgoing and incoming O_c and I_c respectively can be defined by a linear combination of F_c and G_c ,

$$I_c = O_c^* = (G_c - iF_c)e^{i\rho_c} \qquad 2.56$$

where ρ_c is Coulomb phase shift related to the orbital angular momentum number ℓ_c and η_c by

$$\rho_c = \sum_{n=1}^{\ell_c} \tan^{-1}\frac{\eta_c}{n} \qquad 2.57$$

Asymptotically I_c and O_c have the following behavior,

$$I_c^* = O_c \simeq \exp i\,(k_c r_c - \frac{1}{2}\ell_c\pi - \eta_c \ln 2k_c r_c) \qquad 2.58$$

The radial wave function of Equation 2.54 can be written as a linear combination of I_c and O_c ,

$$\Psi = \sum_c \frac{1}{\sqrt{v_c}} (A_c I_c - B_c O_c)\psi_c \qquad 2.59$$

where A_c and B_c are amplitude coefficients, v_c is chosen so that $\frac{I_c}{\sqrt{v_c}}$ corresponds to unit flux.

In terms of the collision matrix $U_{cc'}$ (La 58), the expansion coefficients of Equation 2.59 are related to each other by,

$$B_c = \sum_{c'} U_{cc'} A_{c'} \qquad 2.60$$

In a nuclear reaction we have an incident beam (plane wave) of a given pair of particles α , and an outgoing wave of some pair α' observed in a direction (θ,ϕ) relative to the incident beam. The total wave function can be written then as,

$$\Psi = \Psi_{inc} + \Psi_{reac} \qquad 2.61$$

The incident wave function is described by

$$\Psi_{inc} = \Phi_\alpha X_{sm_s} \exp(ik_\alpha Z_\alpha)$$

$$= \Phi_\alpha X_{sm_s} \sqrt{4\pi} \sum_{\ell=0}^{\infty} \sqrt{2\ell+1}\, j_\ell(k_\alpha r_\alpha) i^\ell Y_{\ell,0}(\theta,\phi) \qquad 2.62$$

At very large distances, when the Coulomb fields of the target and projectile are completely screened, the radial part $j_\ell(k_\alpha r_\alpha)$ of Equation 2.62 can be expressed in terms of the incoming and outgoing waves by

$$j_\ell(k_\alpha r_\alpha) \simeq (k_\alpha r_\alpha)^{-1} F_\ell(k_\alpha r_\alpha)$$

$$= (2k_\alpha r_\alpha)^{-1} i(I_\ell - O_\ell) \qquad 2.63$$

Now equation 2.62 can be written as

$$\Psi_{inc} = \Phi_\alpha \sum_{J=0}^{\infty} \sum_{m_J=-J}^{+J} \sum_{\ell=|J-S|}^{J+S} ik_\alpha^{-1} \pi \frac{1}{2}$$

$$<\ell s\ 0\ m_s | Jm_J> \sqrt{2\ell+1}\ r_\alpha^{-1}$$

$$\sum_{m_\ell=-\ell'}^{\ell} \sum_{m_s,=-s'}^{s'} <\ell s m_\ell, m_s, | Jm_J> (I_\ell - O_\ell) i^\ell Y_{\ell m_\ell} X_{s m_s,} \qquad 2.64$$

where the Clebsch-Gordan coefficients $<\ell s O m_s | Jm_J>$ and $<\ell' s' m_\ell, m_s, | Jm_J>$ are the coupling and decoupling coefficients of the function $Y_{\ell,0}$ and $X_{sm_s'}$ respectively. Using equation 2.52, Equation 2.64 becomes,

$$\Psi_{inc} = \sum_J \sum_{m_J} \sum_\ell <\ell s O m_s | Jm_J> \sqrt{2\ell+1}\ ik_\alpha^{-1} \sqrt{\pi}$$

$$(I_\ell - O_\ell)\ \psi_c \qquad 2.65$$

Since Ψ_{reac} contains only outgoing waves, the coefficients A_c of the total wave function are the coefficients of the incoming waves in Eqn. 2.65

$$A_c \equiv A_{\alpha s \ell}^{Jm_J} = ik^{-1} \sqrt{\pi v_\alpha} <\ell s O m_s | Jm_J> \sqrt{2\ell+1} \qquad 2.66$$

for α, s and m_s of the incident beam and $A_c = 0$ for all other channels.

The amplitude $B_{c'}$ of the outgoing waves is given by equation 2.60,

$$B_{c'} \equiv B^{Jm_J}_{\alpha's'\ell'} = ik^{-1}\sqrt{\pi v_c} \sum_{\ell=|J-s|}^{J+s} \langle \ell s 0 m_s | J m_J \rangle$$

$$\sqrt{2\ell+1}\; U^J_{\alpha s\ell;\alpha's'\ell'} \qquad 2.67$$

By means of Eqns. 2.68, 2.65 and 2.61 we can write Ψ_{reac} as,

$$\Psi_{reac} = \sum_c \sum_{c'} (\delta_{cc'} - U_{cc'}) A_{c'} O_{c'} \qquad 2.68$$

The Kroneker-delta function $\delta_{cc'}$ occurs in this expression because the incident plane wave contains outgoing as well as incoming waves.

The various possible cross-sections are given by Ψ_{reac}. Since the actual detectors in the laboratory are presumed to select a given pair of particles in a given state of excitation and traveling in a direction θ,ϕ, then we can write Ψ_{reac} in the form,

$$\Psi_{reac} \equiv i \sum_{\alpha',s',m_{s'}} k_\alpha^{-1} \left(\frac{v_\alpha}{v_{\alpha'}}\right)^{\frac{1}{2}} r_{\alpha'}^{-1}\, e^{ik_{\alpha'}r_{\alpha'}}$$

$$\Phi_{\alpha'}, X_{s'm_{s'}}, q_{\alpha's'm_{s'}}; {}_{\alpha sm_s}(\theta,\phi) \qquad 2.69$$

Comparing Eqns. 2.69 and 2.68 we get,

$$q_{\alpha's'm_{s'}};{}_{\alpha sm_s}(\Theta,\phi) = -\sum_{J=0}^{\infty} \sum_{m_J=-J}^{+J} \sum_{\ell=|J-s|}^{J+s} \sum_{\ell'=|J-s'|}^{J+s'}$$

$$\sum_{m_{\ell'}=-\ell'}^{\ell'} \sqrt{\pi(2\ell+1)}\, \langle \ell s 0 m_s | J m_J \rangle$$

$$<\ell' s' m_{\ell'}, m_{s'} | J m_J> (\delta_{\alpha\alpha'} \delta_{ss'} \delta_{\ell\ell'} - U^J_{\alpha' s' \ell', \alpha s \ell})$$

$$i^{\ell'} Y_{\ell' m_{\ell'}} (\theta, \phi) \qquad 2.70$$

The differential cross-sections for the process $\alpha \to \alpha'$ is given by the following expression,

$$\frac{d\sigma_{\alpha\alpha'}}{d\Omega} = k_\alpha^{-2} \sum_{m_s=-s}^{s} \sum_{m_{s'}=-s'}^{s'} \sum_{s=|I-i|}^{I+i} \sum_{s'=|I'-i'|}^{I'+i'}$$

$$\frac{1}{(2I+1)(2i+1)} \left| q_{\alpha' s' m_{s'}; \alpha s m_s} (\theta, \phi) \right|^2 \qquad 2.71$$

The last expression can be written in a more convenient form (Ba 61)

$$\frac{d\sigma_{\alpha\alpha'}}{d\Omega} = \frac{1}{k_\alpha^2} \sum_{L=0}^{\infty} B_L(\alpha, \alpha') \, P_L(\cos\theta) \qquad 2.72$$

where $P_L(\cos\theta)$ is Legendre polynomial and $B_L(\alpha, \alpha')$ is given by,

$$B_L(\alpha, \alpha') = \sum_{m_s, m_{s'}, s, s', J_1, J_2, \ell_1, \ell_2, \ell_1', \ell_2'}$$

$$\frac{(-)^{s-s'}}{4(2I+1)(2i+1)} i^{\ell_1 - \ell_2 - L} Z(\ell_1 J_1 \ell_2 J_2; sL)$$

$$i^{\ell_1' - \ell_2' - L} Z(\ell_1' J_1 \ell_2' J_2, sL) \times \mathrm{Re}[(\delta_{\alpha\alpha'} \delta_{\ell_1 \ell_1'} \delta_{ss'} -$$

$$U^{J_1}_{\alpha' s' \ell_1'; \alpha s \ell_1})^* (\delta_{\alpha\alpha'} \delta_{ss'} \delta_{\ell_2 \ell_2'} - U^{J_2}_{\alpha' s' \ell_2'; \alpha s \ell_2})] \qquad 2.73$$

where the Z's are the Z coefficients.

The collision matrix components are complex numbers (Vo 68) which vary rapidly with energy. In addition there is no correlation between the variation with energy of different components of the collision matrix. Consequently when we average the cross-section over an energy interval, we can ignore all cross terms between various components, so each absolute square of the collision matrix components takes the form:

$$\overline{\left|U^{J}_{\alpha' s' \ell', \alpha s \ell}\right|^2} = \frac{T_{\ell}(\alpha) T_{\ell'}(\alpha')}{\sum_{\alpha'' \ell'' s''} T_{\ell''}(\alpha'')} \qquad 2.74$$

in which we used the optical model transmission functions of Equation (2.50). If we take $d\bar{\sigma}_{\alpha\alpha'}/d\Omega$ from Equation (2.72), making use of Eqns. (2.72) and (2.74) we get,

$$\frac{d\bar{\sigma}_{\alpha\alpha'}}{d\Omega} = \sum_{L} \frac{1}{4k_{\alpha}^{2}} \sum_{J\pi} \frac{1}{(2I+1)(2i+1)} \{\sum_{s\ell} T_{\ell}(\alpha)\}$$

$$\sum_{s'\ell'} \{ \frac{T_{\ell'}(\alpha')}{\sum_{\alpha''\ell''s''} T_{\ell''}(\alpha'')} \} Z(\ell J \ell J; sL) Z(\ell' J \ell' J; s' L)$$

$$(-)^{s-s'} P_{L}(\cos \theta) \qquad 2.75$$

The transmission function can be obtained from the corresponding phase shifts using Eqn. (2.50). These phase shifts are obtained from the solution of the radial scattering Schrodinger Equation with the appropriate optical model potential. The solution of these equations $\chi_{\ell j}(r)$ has the boundary conditions (Sm 65)

1) $\chi_{\ell j}(0) = 0$

2) $\chi_{\ell j}(r) \simeq a(F_\ell + iG_\ell) + b(F_\ell - iG_\ell)$

$$= F_\ell - \beta_{\ell j}(F_\ell - iG_\ell) \qquad 2.76$$

with $a = \frac{1}{2}$ and $b = \frac{1}{2}(1-2\beta_{\ell j})$ 2.77

The transmission functions are then written as,

$$T_{\ell j} = 1 - \left|\frac{b}{a}\right|^2 = 1 - |1-2(Re\beta_{\ell j} + iIm\beta_{\ell j})|^2$$

$$= 4\,[Re\beta_{\ell j} - [(Re\beta_{\ell j})^2 + (Im\beta_{\ell j})^2]$$

$\beta_{\ell j}$ is determined by solving

$$\frac{\chi_{\ell j}(r_1)}{\chi_{\ell j}(r_2)} = \frac{F_\ell(r_1) - \beta_{\ell j}[F_\ell(r_1) - iG_\ell(r_1)]}{F_\ell(r_2) - \beta_{\ell j}[F_\ell(r_2) - iG_\ell(r_2)]} \qquad 2.78$$

As the excitation energy of the compound nucleus increases and reaches the continuous region, or if spin, parity, and excitation energies of the residual nucleus are not known, we must include the level density expressions into any expression for the transmission functions. The density $\rho(E^*,I)$ of states of spin I of a nucleus is usually assumed to depend on the excitation energy E^* of the states and their spin, but to be independent of the parity and other properties (Vo 68). It is a common practice to assume that the energy dependence and spin dependence are separate factors (Vo 68),

$$\rho(E^*,I) = \rho(E^*)[(2I+1)e^{-I(I+1)/2\sigma^2}] \qquad 2.79$$

where σ is called the spin cut off parameter, is proportional to $(E^*)^{\frac{1}{4}}$, $\sigma \simeq 2.5$ for $E^* = 10$ MeV (Da 68).

It is found (Da 68) that to a good approximation, the $\rho(E^*)$ is given by (Ne 56),

$$\rho(E^*) = \frac{dN(E^*)}{dE^*}$$

$$= \frac{1.15b}{\sqrt{E^*}} \exp\left[2.3(a+b)\sqrt{E^*}\right] \qquad 2.80$$

The any transmission function $T_{\ell'}$ should be replaced by

$$\sum_{s'\ell'} T_{\ell'} \rightarrow \sum_{\ell'} \rho(I) \int_{E_1}^{E_2} T_{\ell'}\rho(E^*)dE^* \qquad 2.81$$

where E_1 is the maximum energy of the discrete region, $E_2 = E_p^{max}$.

CHAPTER 3

THE EXPERIMENT

3.1 The Experimental Set-Up:

The most accurate measurement of neutron energy is by means of time-of-flight technique. This technique is characterized by good resolution over a large energy range. The idea is based on measuring the energies of neutrons by individually timing their flight over an accurately measured path. It is of great importance to accurately fix two time points,

a) The zero-time point, which corresponds to the time at which the particle starts its flight path, and

b) The stop-time point, which corresponds to the detection of the neutron.

The most general technique (Ne 59) for obtaining a zero time is that of the pulsed beam which can give a zero time independent of the reaction mechanism. In this method the beam of the incident particles which initiate the reaction is pulsed onto the target for a time short compared to the flight time to be measured and at such a rate that the longest flight time of interest can be measured before the next beam reaches the target. Since the time of flight of a several MeV neuterons is in the nano-second region, very short ion bursts of high intensity are required. Using both pre-acceleration pulsing and post-acceleration compression, the University of Alberta 5.5 MeV Van de Graaff accelerator is able to satisfy these requirements.

An ion source located within the high voltage terminal is used to ionize deuterium gas by 125 MHz source oscillator and a d-c ion beam is extracted by means of a probe electric field. The beam starts to accelerate downward. An Einsel lens and Terminal Analysis magnet are used to focus the beam which can then be pulsed by two sets of R.F. deflection plates set at right angles to each other and driven 90° out of phase by a 1 MHz oscillator. These R.F. deflection plates sweeps the beam in an elliptical path over a 1/16 inch aperture, producing a beam pulse of 10 ns width, which after focusing by Focus 3, is analysed by a 90° magnet to reflect the desired energy (momentum). The beam then passes through a pair of energy stabilizing slits 57 inches away from the analysing magnet. These slits feed the corona current central system which stabilizes the energy. A magnetic quadrupole lens is used to focus the beam inside the first stage of the Mobley compression system. The first stage of the Mobley system is a pair of deflection plates fed with a phase locked R.F. oscillator of 10 MHz. Phase information is supplied to the oscillator from a cylindrical pick-off in the beam tube just before the R.F. plates. The second stage is a 90°, 75 inch magnet whose focal points are at the target and the R.F. plates. The beam pulse is swept by the R.F. field such that the particles leaving the deflector plates first take the longest paths through the magnet while those leaving last take the shortest paths. If the phase and amplitude of the deflector are properly adjusted, all particles will arrive at the target at almost the same time. A final beam pulse with width of 0.4 ns can be obtained at the target. A schematic diagram of the beam handling system together with the Mobley system is shown in Fig. 3-1.

FIGURE 3-1

BEAM TRANSPORT SYSTEM

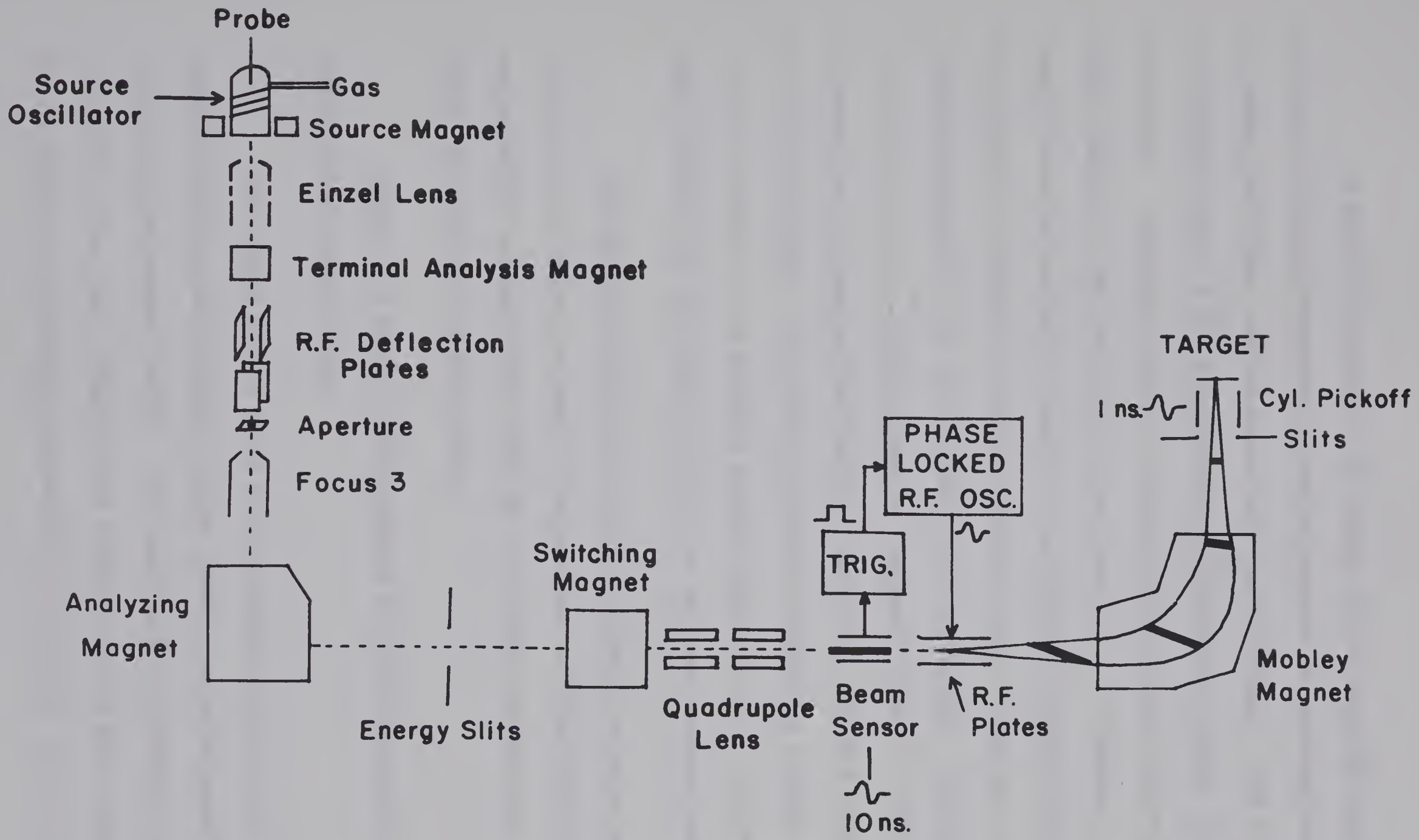
Probe
Source
Oscillator
Gas
Source Magnet
Einzel Lens
Terminal Analysis Magnet
R.F. Deflection
Plates
Aperture
Focus 3
Analyzing
Magnet
Energy Slits
Switching
Magnet
Quadrupole
Lens
PHASE
LOCKED
R.F. OSC.
TRIG.
Beam
Sensor
10 ns.
R.F.
Plates
TARGET
1 ns.
Cyl. Pickoff
Slits
Mobley
Magnet

In order to determine the energy of the outgoing neutron groups, a time-of-flight spectrometer is used to measure the neutrons velocities by timing the flight over an accurately known distance. The stop signal is obtained from a 3 cm. long cylinderical capacitor placed 30 cm. before the target. The start signal is obtained from the main neutron detector, which consists of NE 218 liquid scintillator in a 3" diameter by 1/2" long quartz container optically coupled to an RCA-4522 photomultiplier tube. The detector is fixed to a remote-controlled cart. This cart can be moved through distances of 1.0 to 6.3 meters from the target. The angle between the detector and the incident beam is changeable from 0 to 150°. In order to normalize the angular distribution a detector used as a monitor is held at a fixed position. The monitor detector consists of a Naton phosphor optically coupled to an RCA-8575 photomultiplier tube. The monitor electronics system uses the same stop pulse as the main detector system.

The capacitor pick-off is used to provide the stop signal instead of the detector pulse, to avoid a large number of false starts (CH 61) corresponding to beam bursts which do not produce any neutrons. This will reduce the dead time of the system.

Figure 3-2 shows a block diagram for the electronics of the time-of-flight spectrometer.

The output of the anode of the photomultiplier tube is fed to a constant-fraction-pulse-height-trigger (CFPHT), which triggers at 1/10 of the input pulse height (Ge 67). This was found to eliminate the jitter (or walk) of the start trigger point relative to the stop trigger point due to change in the detector pulse size. The ratio 1/10 is chosen for

FIGURE 3-2

TIME-OF-FLIGHT ELECTRONICS

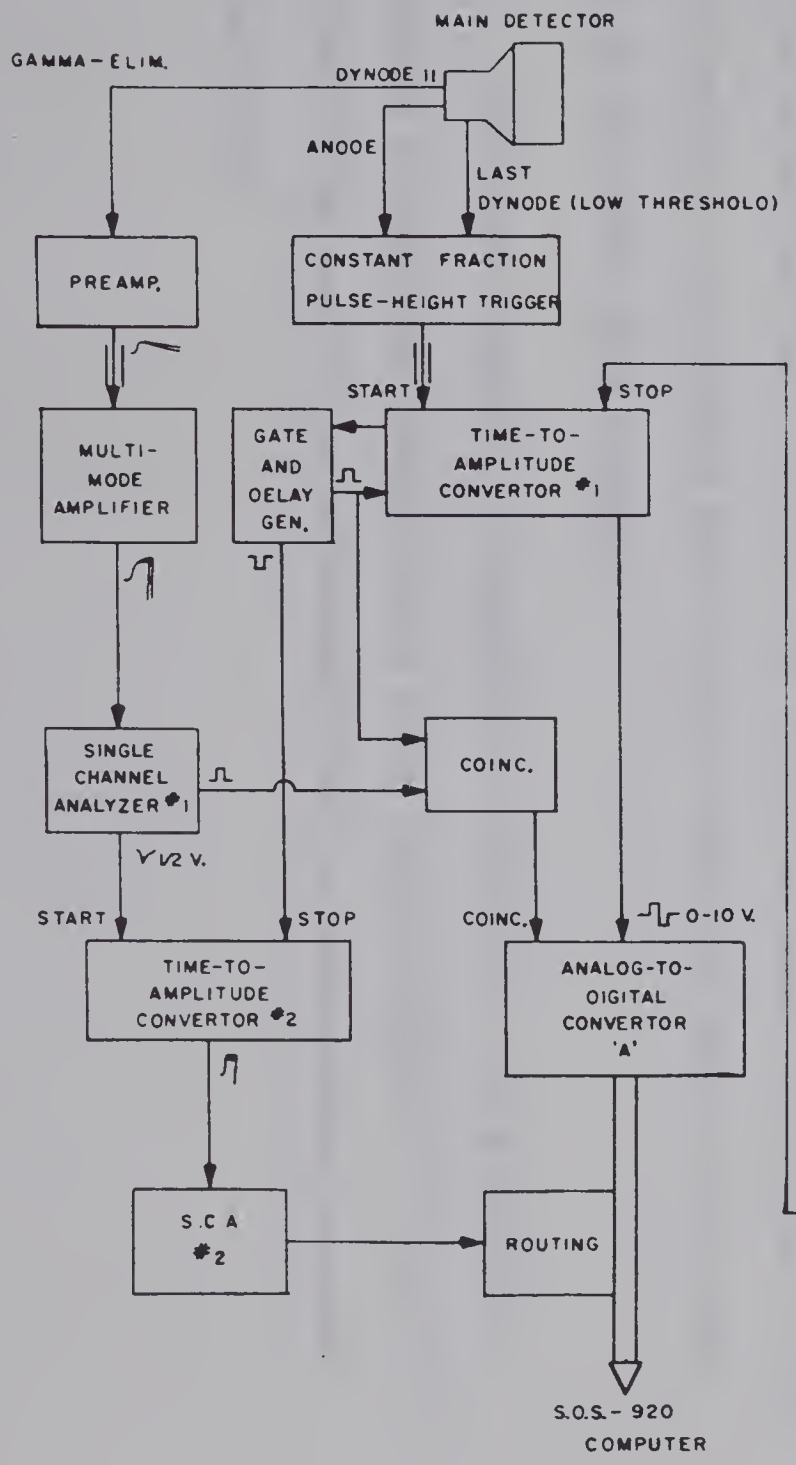
MAIN DETECTOR
GAMMA-ELIM.
DYNODE II
ANOOE
LAST
DYNODE (LOW THRESHOLO)
PREAMP.
CONSTANT FRACTION
PULSE-HEIGHT TRIGGER
START
STOP
MULTI-
MODE
AMPLIFIER
GATE
AND
OELAY
GEN.
TIME-TO-
AMPLITUDE
CONVERTOR #1
SINGLE
CHANNEL
ANALYZER #1
COINC.
+12 V.
START
STOP
COINC.
0-10 V.
TIME-TO-
AMPLITUDE
CONVERTOR #2
ANALOG-TO-
OIGITAL
CONVERTOR
'A'
S.C.A
#2
ROUTING
S.O.S.-920
COMPUTER

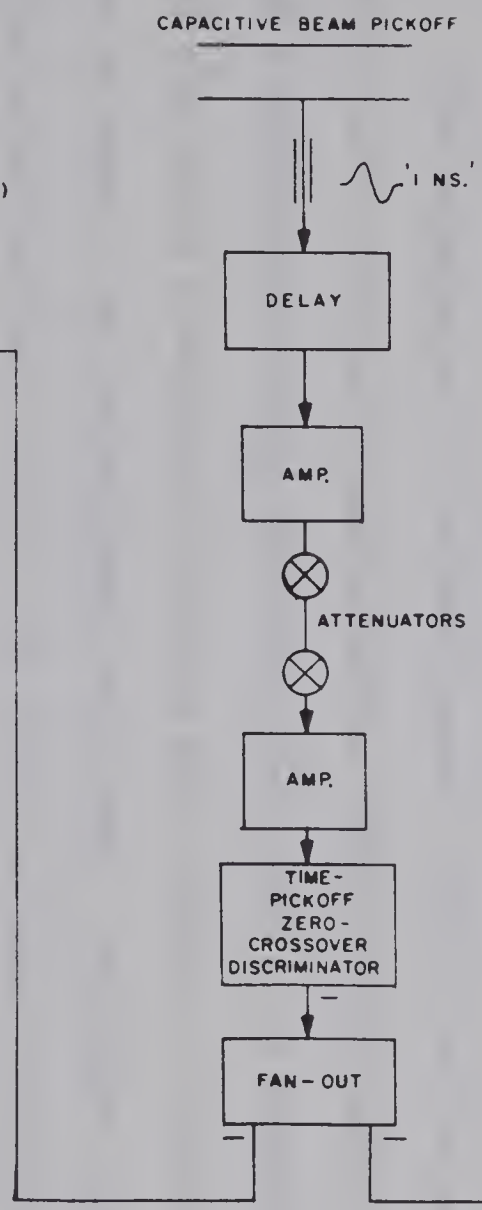
CAPACITIVE BEAM PICKOFF
'1 NS.'
DELAY
AMP.
ATTENUATORS
AMP.
TIME-
PICKOFF
ZERO-
CROSSOVER
DISCRIMINATOR
FAN-OUT

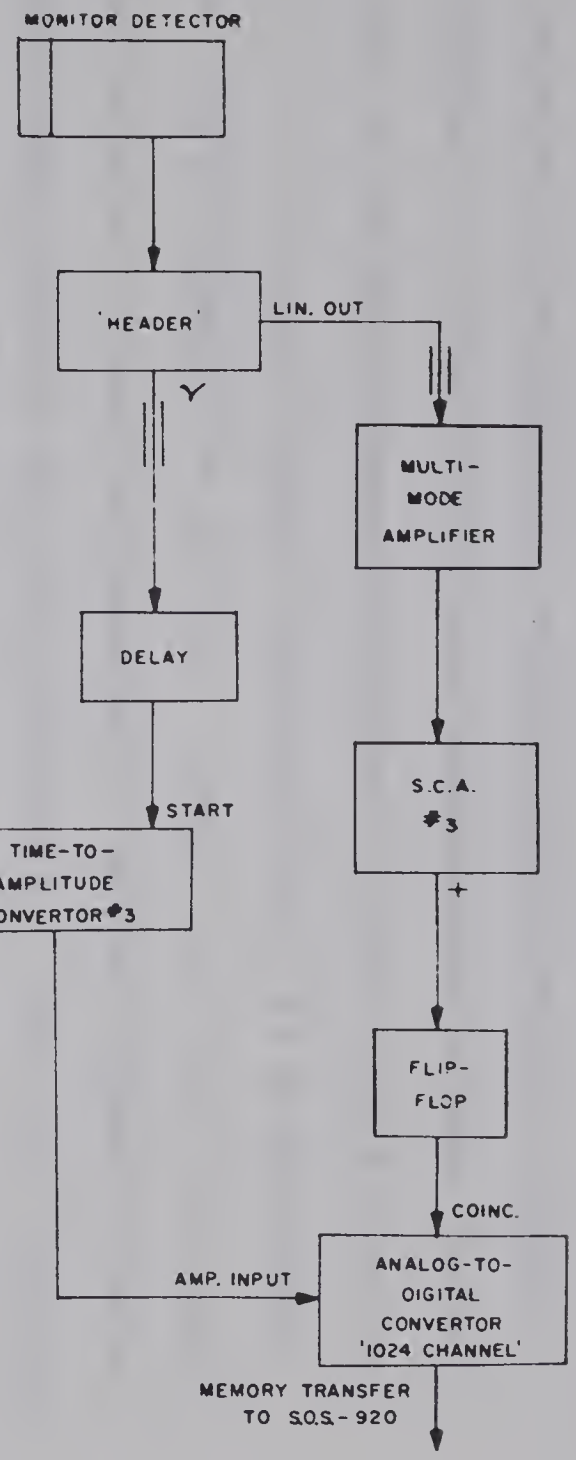
MONITOR DETECTOR
'HEADER'
LIN. OUT
MULTI-
MODE
AMPLIFIER
DELAY
STOP
START
TIME-TO-
AMPLITUDE
CONVERTOR #3
S.C.A.
#3
FLIP-
FLOP
COINC.
AMP. INPUT
ANALOG-TO-
OIGITAL
CONVERTOR
'1024 CHANNEL'
MEMORY TRANSFER
TO S.O.S.-920

the best time resolution. The output of the C.F.P.H.T. provides the start pulse for an Ortec model 437 Time-to-Amplitude-Converter (T.A.C.) #1. The output of the capacitive beam pick off is fed (after delayed and amplified), to a Time-Pickoff-Zero-Crossover-Discriminator (Ge 67a). The output of the Zero-Crossover-Discriminator is used as the stop pulse of T.A.C. #1 in the main detector circuit and T.A.C. #3 in the monitor circuit. It is necessary for the T.A.C. output to be timed with respect to start pulse, so a signal corresponding to the start signal is fed to a gate-and-delay generator and back into the T.A.C. The T.A.C. gives an output pulse only when the delayed start pulse is sensed. The output of T.A.C. #1 is fed to an Analog-to-Digital-Converter 'A' (A.D.C.A.) which in turn feeds the S.D.S.-920 on-line computer.

The elimination of the back ground γ-rays from the neutron spectrum, can be achieved by measuring the time interval (using T.A.C. #2) between a delayed start pulse and cross-over point of an integrated and clipped slow pulse from dynode 11 of the main detector. This time interval differs by about 25 ns for neutrons and γ-rays. Any pulse identified as a neutron pulse derives a routing unit which increases the address of the neutron pulses to the second 2048 channels while the rest of the pulses remain in the first 2048 channels.

For more reduction of background the A.D.C.A. is gated by a coincidence between the delayed start pulse and the output of S.C.A. #1. The S.C.A. #1 is used to set a threshold for the main neutron detector (see Sec. 3.2).

Due to the nature of the monitor job, the high time resolution and separation of γ-rays are not of great importance. So a simple version of main detector circuit is used for the monitor circuit. The monitor spectrum is stored in a 1024-channel A.D.C. and can be dumped into the computer memory on command. All data are recorded on magnet tape.

3.2. Detector Efficiency:

The detector efficiency should be known in order to calculate the absolute cross-sections. The efficiency of the neutron detector was calculated using a computer code written by Grandy (Gr 67).

The detector efficiency is a function of the detector lower threshold, so the cutoff neutron energy should be measured. Fig. 3-3 shows the block diagram of the circuit used for this purpose. Fig. 3-4 shows a gamma-ray spectrum of ^{22}Na obtained by using the circuit of Fig. 3-3. The lower threshold in electron energy is given by,

$$\text{Lower Threshold} = R \cdot E_c$$

where R is the ratio between the cutoff channel and the channel corresponding to 2/3 of the height of the 0.511 MeV Compton edge, and E_c=340 KeV, is the maximum Compton electron energy. To get the threshold in terms of proton recoil energy instead of electron energy, a response curve of NE 218 scintillator to electrons and protons is required. Such a curve is not available so the data published by Smith et al. (Sm 68) for NE 213, which is quite similar to NE 218, has been used.

FIGURE 3-3

BLOCK DIAGRAM OF CUTOFF ELECTRONICS

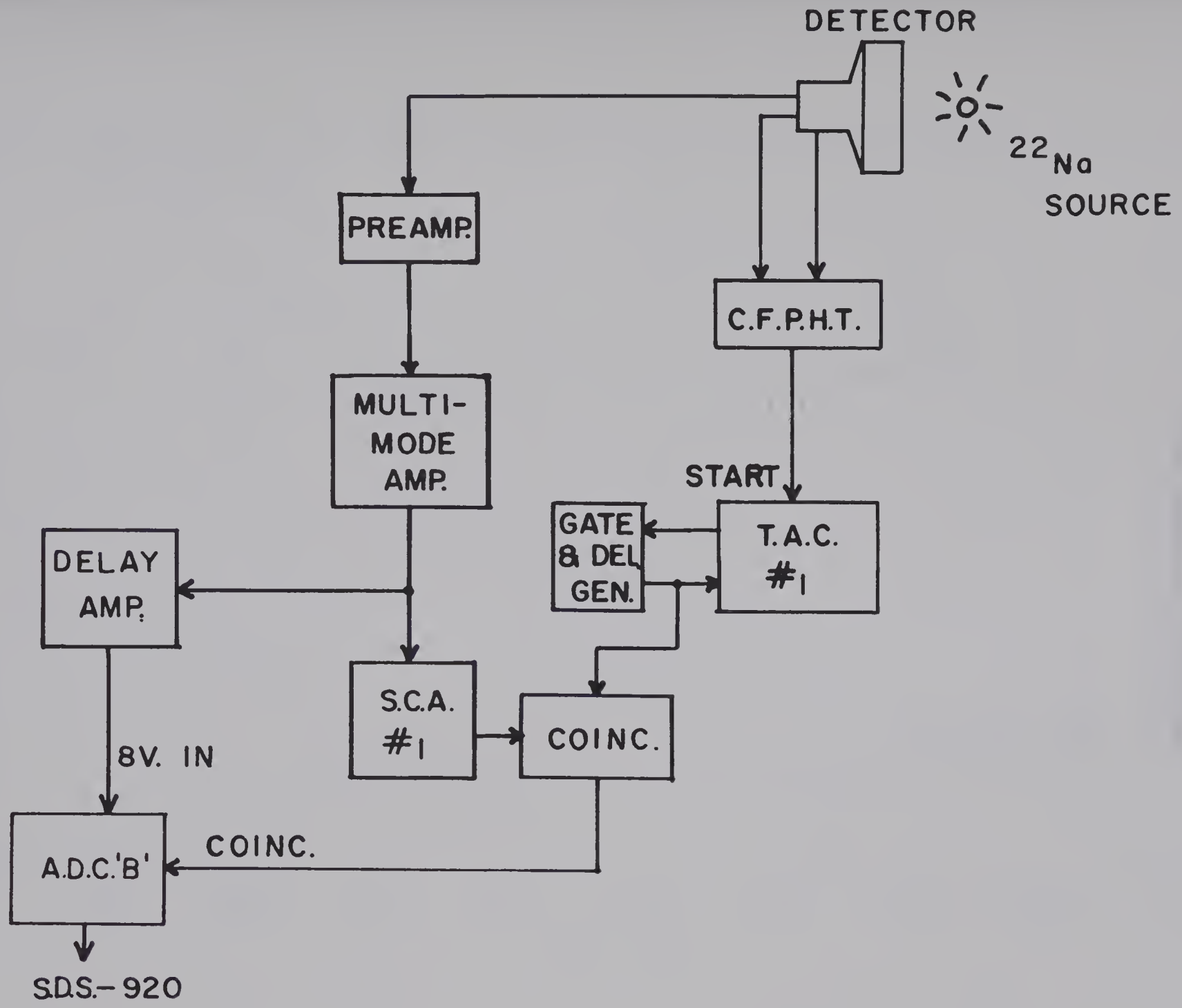
DETECTOR
^{22}Na SOURCE
PREAMP.
C.F.P.H.T.
MULTI-MODE AMP.
START
GATE & DEL GEN.
T.A.C. #1
DELAY AMP.
S.C.A. #1
COINC.
8V. IN
COINC.
A.D.C.'B'
S.D.S.-920

FIGURE 3-4

^{22}Na GAMMA-RAY SPECTRUM

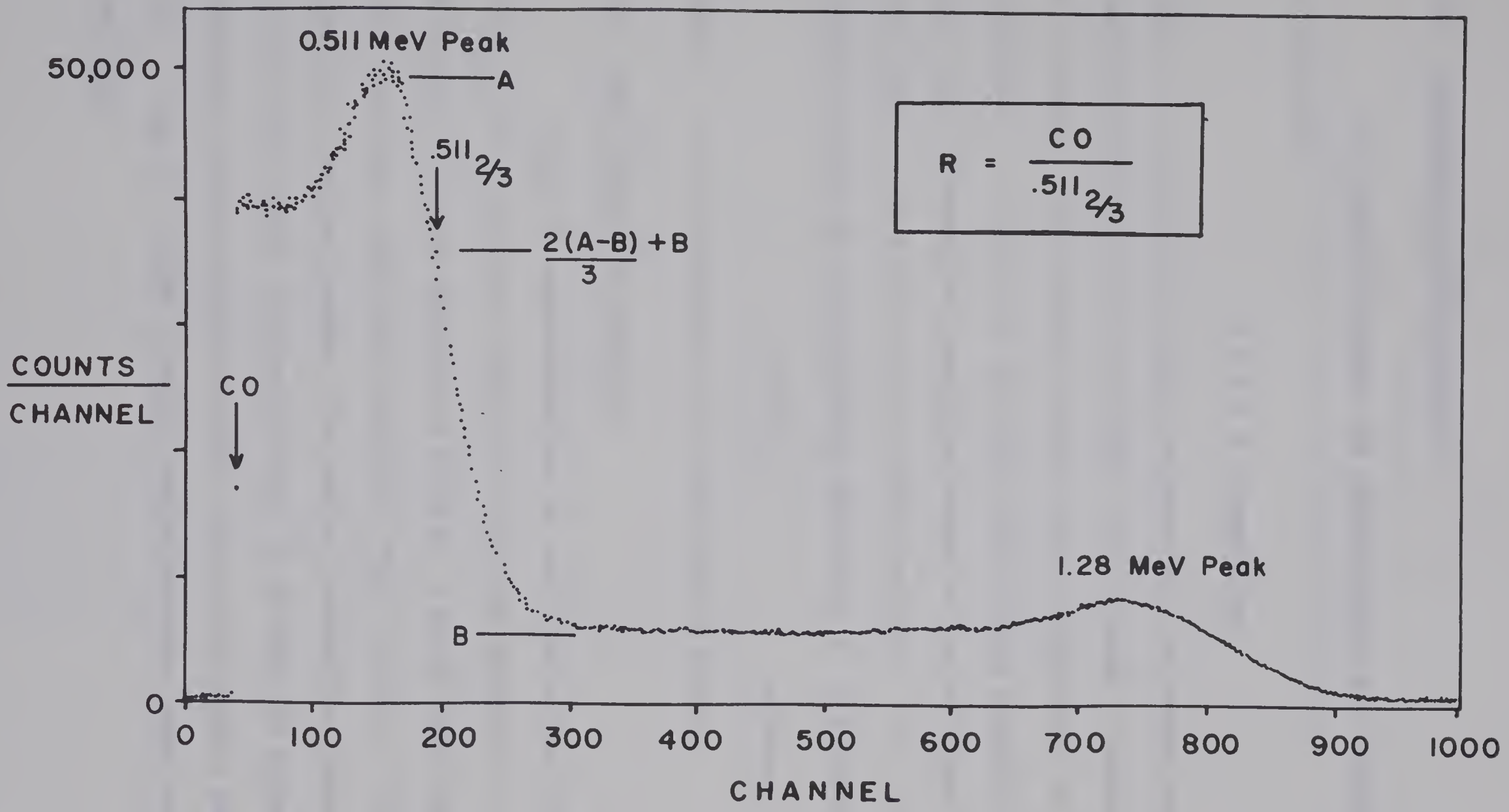
0.511 MeV Peak
A
.511 2/3
2(A-B) + B
3
CO
B
1.28 MeV Peak
R = CO / .511 2/3
50,000
0
COUNTS
CHANNEL
0
100
200
300
400
500
600
700
800
900
1000
CHANNEL

3.3. Calibration of Time Spectra:

The relation between the time-of-flight and channel number is a linear one,

$$T = A + B \times \text{channel no.}$$

where T is the time-of-flight in nano-sec. The channel number of a gamma-ray peak along with its flight time is enough to determine A, if B is known. The electronic circuit shown in Figure 3-5 is used to determine B. The T.A.C. will give output pulses whenever the start-stop time difference is a multiple integer of the oscillator frequency, and the output of the A.D.C. will be a chain of peaks. If d is the average spacing between any two successive peaks then B is given by,

$$B = 10^3/(d \cdot f) \qquad \text{ns/channel}$$

where f is the frequency of the oscillator in Mc/sec.

3.4. The $^{31}P(d,n)^{32}S$ Reaction:

Using the experimental set up described in Sec.(3.1), the $^{31}P(d,n)^{32}S$ reaction has been done at deuteron energies of 4.00 and 5.45 MeV, and flight distance of 6.325 m. A solid target was prepared by evaporating, commercially produced, Zn_3P_2 (purity > 95%) under vacuum onto a tantalum backing. The monitor detector was placed at an angle of -30° with respect to beam direction, at 3m from the target. In each experiment neutron spectrum has been taken in the angular range of 0 to 140°. Fig. 3-6 shows a typical neutron spectrum taken at 60° with 4.0 MeV deuterons.

FIGURE 3-5

BLOCK DIAGRAM OF TIME CALIBRATION ELECTRONICS

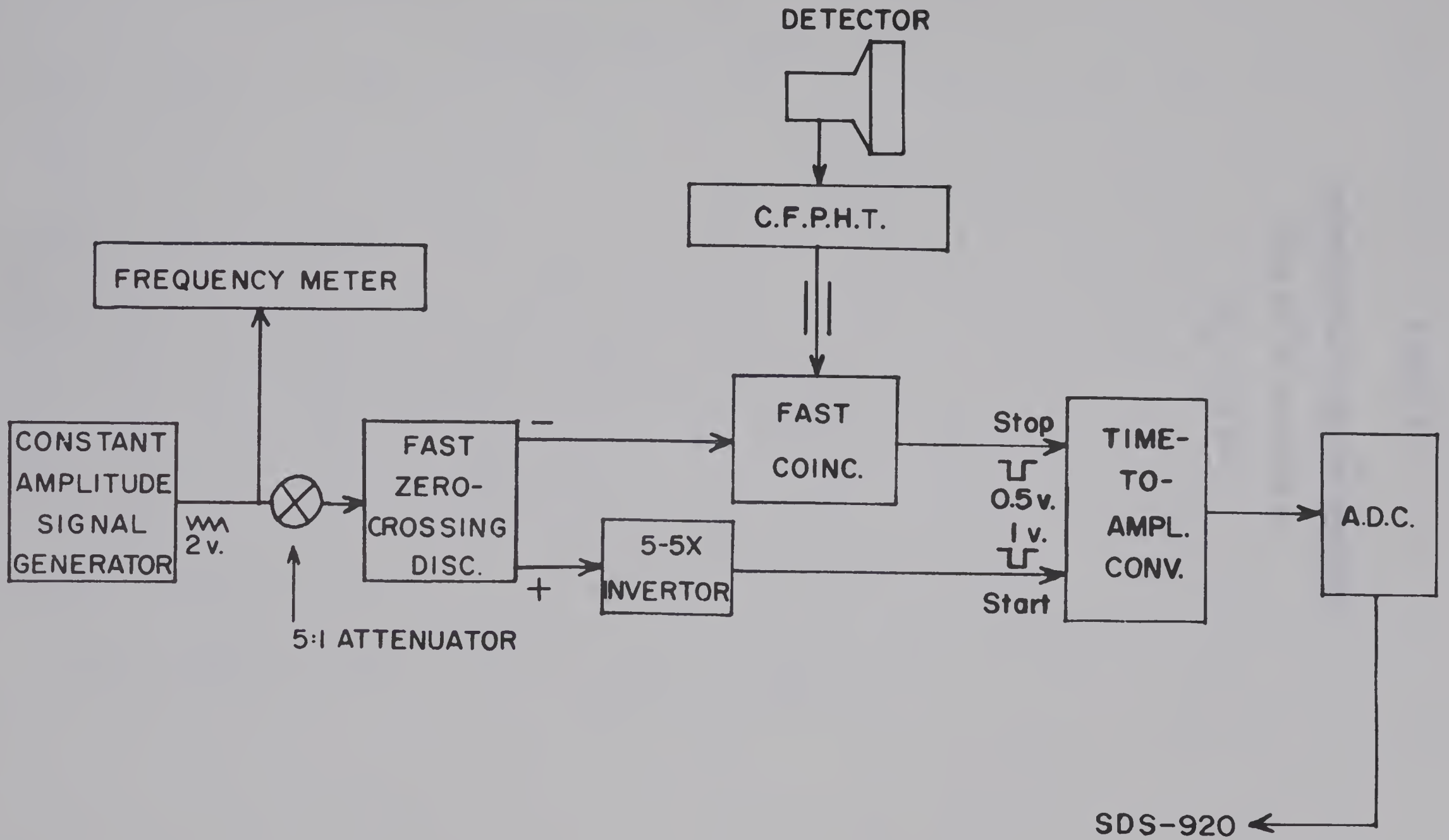
DETECTOR
C.F.P.H.T.
FREQUENCY METER
CONSTANT AMPLITUDE SIGNAL GENERATOR
2 v.
FAST ZERO-CROSSING DISC.
5:1 ATTENUATOR
−
+
5-5X INVERTOR
FAST COINC.
Stop
0.5 v.
1 v.
Start
TIME-TO-AMPL. CONV.
A.D.C.
SDS-920

FIGURE 3-6

NEUTRON TIME-OF-FLIGHT SPECTRUM

$^{31}P(d,n)^{32}S$ REACTION AT

E_d = 4.0 MeV

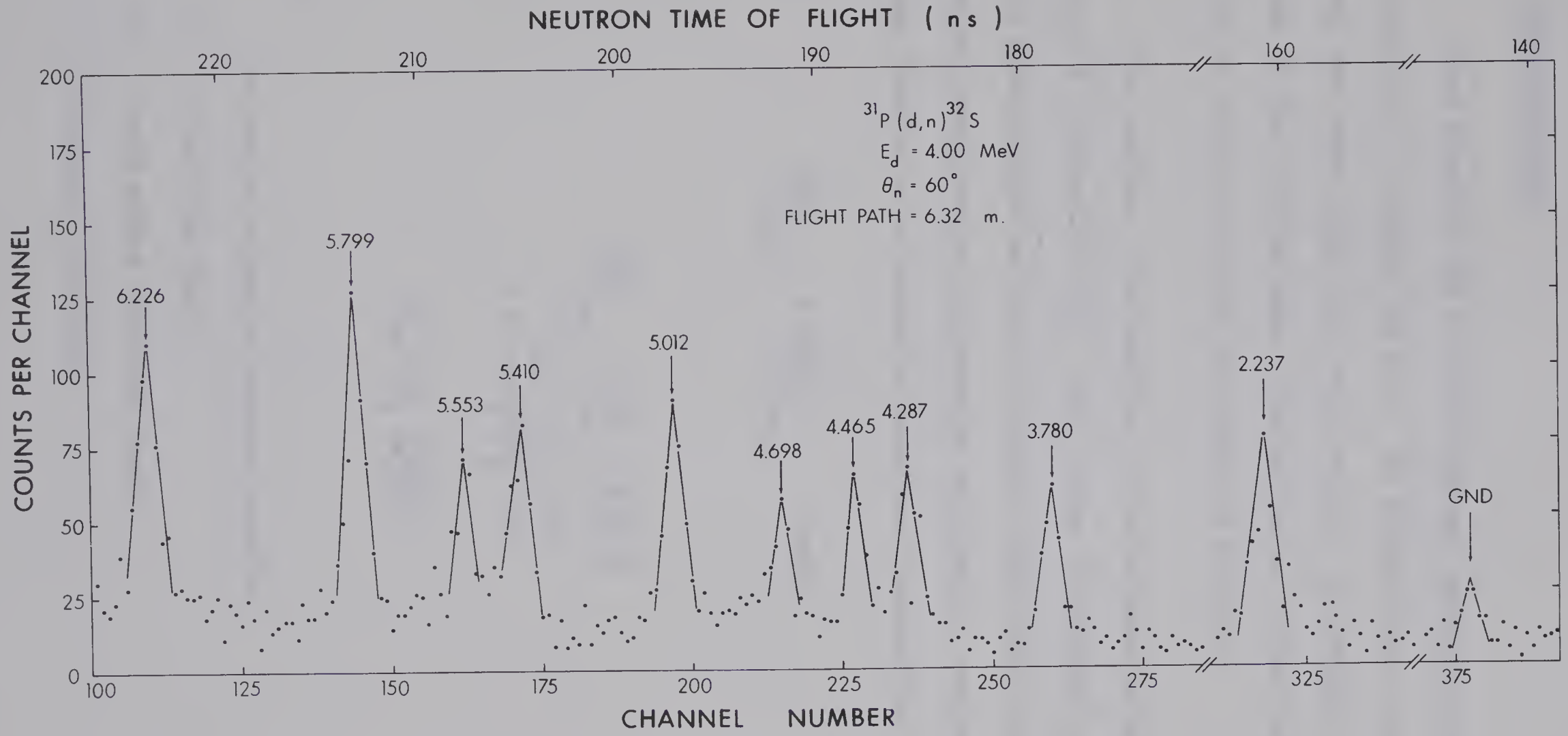
NEUTRON TIME OF FLIGHT (n s)
220
210
200
190
180
160
140
$^{31}P(d,n)^{32}S$
E_d = 4.00 MeV
θ_n = 60°
FLIGHT PATH = 6.32 m.
COUNTS PER CHANNEL
200
175
150
125
100
75
50
25
0
6.226
5.799
5.553
5.410
5.012
4.698
4.465
4.287
3.780
2.237
GND
100
125
150
175
200
225
250
275
325
375
CHANNEL NUMBER

3.5. Cross-Sections:

Peak areas of the 5.45 MeV data are extracted using a computer code written by J.W. Tepel (Te 66). The output of the program is the peak positions and areas along with their errors. The program fails to extract the peaks of the 4.00 MeV data, this may be due to the low statistics of this run, so those peak areas are extracted by hand.

The absolute cross-sections are calculated using computer code written by N. Davison (Da 69). This program is written to calculate the absolute cross-section in the C.M. System taking into consideration time and monitor normalization and detector efficiency. The program uses the following formula to calculate the absolute cross-section,

$$\left(\frac{d\sigma}{d\Omega}\right)_{abs.} = W\left(\frac{d\sigma}{d\Omega}\right)_{rel.} \quad \text{mb/sr}$$

where

$$\left(\frac{d\sigma}{d\Omega}\right)_{rel.} = \frac{A}{A'_m} \cdot \frac{t.t.}{\ell.t.} \frac{1}{\varepsilon}$$

$$W = \frac{1.6 \times \bar{A}'_m \times 10^{14}}{Q\ \Omega\ N}$$

$$A'_m = A_m \frac{t.t.}{m.\ell.t.}$$

where,

A = area of a peak in neutron spectrum

t.t. = true time (sec.)

ℓ.t. = main system live-time (sec.)

ε = detector efficiency

$\overline{A}'_m$ = average of A'_m

Q = average charge (μ Coul.)

Ω = solid angle subtend by the detector

= 1.51×10^{-4} sr at 6.3 m.

N = number of target nuclei per cm^2

A_m = area of a peak in monitor spectrum

m.ℓ.t. = monitor system live-time.

Absolute cross-section for the G.S., 2.23, 3.78, 4.29, 5.55, 5.8, and 6.23 MeV states of ^{32}S are given in Appendix A, Tables A-1 to A-7.

CHAPTER 4

ANALYSIS OF EXPERIMENTAL DATA

4.1 Optical Model Potentials

To carry out the DWBA calculations we need the optical model potentials of all particles involved in the reaction. These optical potentials are expressed by a set of parameters. The general form of the optical potential may be given by:

$$U(r) = V_c(r) - Vf(x_v) + i4a_w w \frac{d}{dx_w} f(x_w)$$
$$-(V_{so} + iw_{so}) \frac{1}{r} \frac{d}{dr} f(x_{so}) \vec{L}\cdot\vec{\sigma} \qquad 4.1$$

$V_c(r)$ is the Coulomb potential of uniformly charged sphere with

$$V_c(r) = \frac{Zze^2}{2R_c} [3 - (\frac{r}{R_c})^2] \qquad r \leq R_c = r_c A^{\frac{1}{3}} \qquad 4.2$$

$$V_c(r) = \frac{Zze^2}{r} \qquad r \geq R_c \qquad 4.3$$

The shapes of the nuclear potential wells are determined by the Woods-Saxon form factor

$$f(x) = (1 + e^x)^{-1} \qquad 4.4$$

where,

$$x_v = \frac{r - r_v A^{\frac{1}{3}}}{a_v} \;,\; x_w = \frac{r - r_w A^{\frac{1}{3}}}{a_w} \qquad 4.5$$

$$x_{so} = \frac{r - r_{so} A^{\frac{1}{3}}}{a_{so}}$$

The parameters r_v, r_w and r_{so} are real, imaginary and spin-orbit

radii respectively; the parameters a_v , a_w and a_{so} are the real, imaginary and spin-orbit diffuseness'. The depths of the potentials are determined by the real v , the imaginary w and the spin-orbit v_{so} .

We see from Equation 4.1 that it contains eleven parameters. These parameters, in general, are functions of energy and atomic mass (Ho 67); so they can be determined by fitting the experimental elastic scattering angular distributions with those obtained from the optical model calculations by varying these parameters until a good fit is obtained. Unfortunately, the set of parameters which gives a good fit is not unique (Le 64, Bo 70) and this contributes to the ambiguity in the deduced spectroscopic factors. So, to determine the optical potentials, necessary for the DWBA calculations for the reaction $^{31}P(d,n)^{32}S$, then elastic scattering data of the different particles should be available at the same energies and on the same nuclei. In the following we will discuss optical model potentials of each particle individually.

a) The Neutron:

The reaction $^{31}P(d,n)^{32}S$ has been done at $E_d = 5.45$ and 4.00 MeV and this yields neutrons with energies ranging from about 12 MeV (for G.S. at 5.45 MeV) to about 4.0 MeV (for 6.223 MeV state at 4.0 MeV). There are no elastic scattering experiments for neutrons on ^{32}S covering this energy range. However, D. Willmor and P.E. Hodgson (Wi 63) analysed a large number of neutron elastic scattering experiments on nuclei with mass numbers starting from that of Si to that of U , at energies from 1 MeV to 15 MeV . They deduced a general dependence of the neutron optical potential parameters on mass number and energy. This dependence is given by:

$$V = 47.01 - 0.267E - 0.00118E^2 \ , \qquad 4.6$$

$$W = 9.52 - 0.53E \ , \qquad 4.7$$

$$r_v = 1.322 - 0.00076A + (4.10^{-6})A^2 - (8.10^{-9})A^3 \ , \qquad 4.8$$

$$r_w = 1.266 - 0.00037A + (2.10^{-6})A^2 - (4.10^{-9})A^3 \ , \qquad 4.9$$

$$a_v = 0.66 \ , \qquad 4.10$$

$$a_w = 0.48 \ . \qquad 4.11$$

where E is the energy of the incident neutron and A is the mass number of the target nucleus.

b) The Deuteron:

Unfortunately no elastic scattering data are available for deuteron with energies of 4.0 and 5.45 MeV on ^{32}S . So the optical model potential parameters given by D.P. Gurd et. al. (Gu 68) have been used. The parameters are given in Table 4-1. These parameters have been extracted from elastic scattering of deuterons on ^{28}Si . The set as given in Table 4-1 was used to analyse the 5.45 MeV data. A small change in w was necessary for the 4.00 MeV data to keep the spectroscopic factors consistent. The value for w used in this case was 25 MeV .

c) The Proton:

The proton potential is a bound particle potential which is a real potential (see Sec. 2-2) . The depth of the proton potential is adjusted by the computer code used for DWBA calculations (see Secs. 2-2 and 4-3).

TABLE 4-1

OPTICAL MODEL PARAMETERS

Parameter†	Deuteron	Alpha*	Proton*
V(MeV)	107.0	200.0	54.0
r_v(fm)	1.18	1.69	1.25
a_v(fm)	0.9	0.576	0.65
w(MeV)	18.5	15.625	10.0
r_w(fm)	1.7	1.69	1.25
a_w(fm)	0.4	0.576	0.75
r_c(fm)	1.25	1.69	1.25
V_{so}(MeV)	- -	- -	7.0

† For Definition see Eqs. 4.1-4.5

* For HF Calculations Only

4.2 The HF Calculations

The contribution of the compound nucleus process to the (d,n) reaction has been calculated using the statistical model by the computer code Hauser-Feshbach written by W.R. Smith (Sm 65) and modified by N. Davison (Da 68) to include the level density formula (see Sec. 2.3).

The output of this program (differential cross-section) was very sensitive to any change in the level density parameters a and b (eq. 2.80) of the (d,n) channel, while it was completely insensitive to any change in the parameters of the other channels. The parameters of the (d,n) channel calculated by least squares method and the standard deviation in these parameters were used to define the region in which the HF calculations are quite certain. Table 4-2 represents the values of the parameters of all possible channels along with the standard deviations σ_a and σ_b in a and b respectively.

It was also found that the output of the program overestimated the magnitude of the differential cross-section. To overcome this a state which shows a pure compound nucleus pattern in its angular distribution was used to normalize the cross-section. The normalization factor for the 4.0 MeV experiment was 0.3 and 0.1 for the 5.45 MeV experiment.

4.3 DWBA Calculations

The DWBA calculations have been carried out by the computer code DWUK written by P.D. Kunz (Ku 67). The optical potentials defined in Sec. (4.1) with the parameters of Table 4-1 were used to carry out the calculations. The potentials are local with a lower

TABLE 4-2

LEVEL DENSITY PARAMETERS

Parameter	(d,d)	(d,n)	(d,p)	(d,α)	(d,He^3)
a	-1.019	-1.040	-0.226	-0.243	-1.131
σ_a		0.141	0.073		
b $(MeV)^{-\frac{1}{2}}$	0.943	0.826	0.745	0.616	0.910
σ_b		0.063	0.034		

The level density is given by $\log N(E_x) = a + b\sqrt{E_x}$.

σ_a and σ_b are standard deviations in a and b respectively.

cutoff of zero fm in the radial integral and a value of 0.621 fm for finite range corrections.

Figures 4-1-4-14 show the experimental data and both the DWBA and HF predictions for the differential cross-sections for the ^{32}S levels.

Most of the levels show a strong direct pattern specially at 5.45 MeV deuteron energy. The 4.29 MeV state is the only state which shows a compound nucleus pattern at both deuteron energies. The solid curve is DWBA normalized to the main peak. The curves which are marked with "X" represent the HF alone. The rhombuses represent the experimental cross-section, and the vertical bars represent the statistical errors.

Table 4-3 summarizes the DWBA predictions for the ℓ_p-values of ^{32}S energy levels understudy along with those obtained from previous (d,n) work carried out by Ferguson et. al. (Fe 68), (He^3,d) work by Graue et. al. (Gr 68) and Morrison (Mo 70) and those compiled by Endt and Van der Leun (En 67) before 1967.

The figures of the 2.237, 4.29 and 5.55 MeV states at 4.0 MeV deuteron energy and that of the 4.29 MeV state at 5.45 MeV deuteron energy have two HF curves. The upper curve is the HF prediction with level density parameters $a-\sigma_a$ and $b-\sigma_b$ while the lower one with $a+\sigma_a$ and $b+\sigma_b$.

4.4 Spectroscopic Factors

The spectroscopic factors for ^{32}S levels under study have been calculated according to (neglecting the interference between direct and

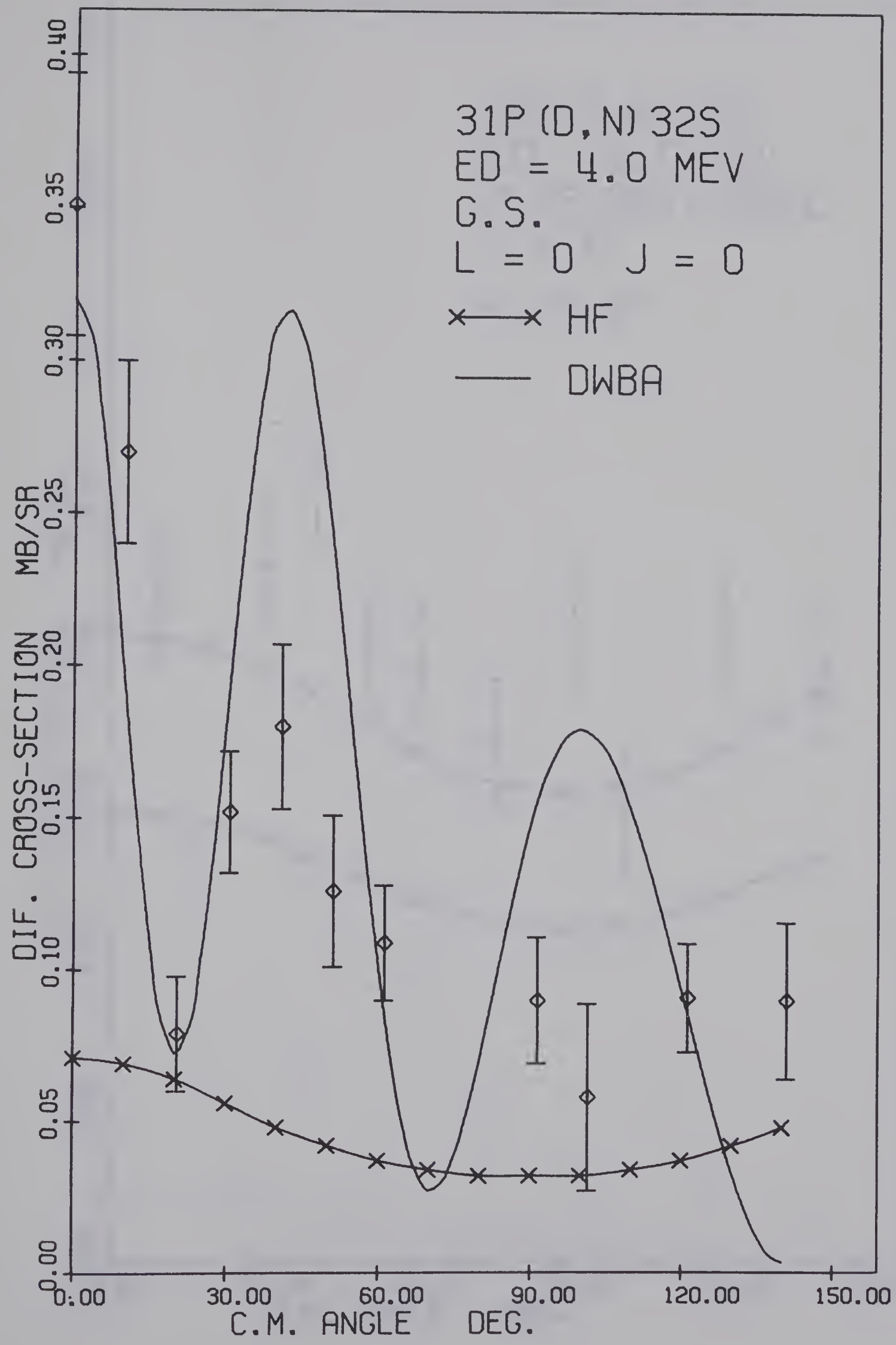
31P (D, N) 32S
ED = 4.0 MEV
G.S.
L = 0 J = 0
HF
DWBA
DIF. CROSS-SECTION MB/SR
0.00
0.05
0.10
0.15
0.20
0.25
0.30
0.35
0.40
0.00
30.00
60.00
90.00
120.00
150.00
C.M. ANGLE DEG.

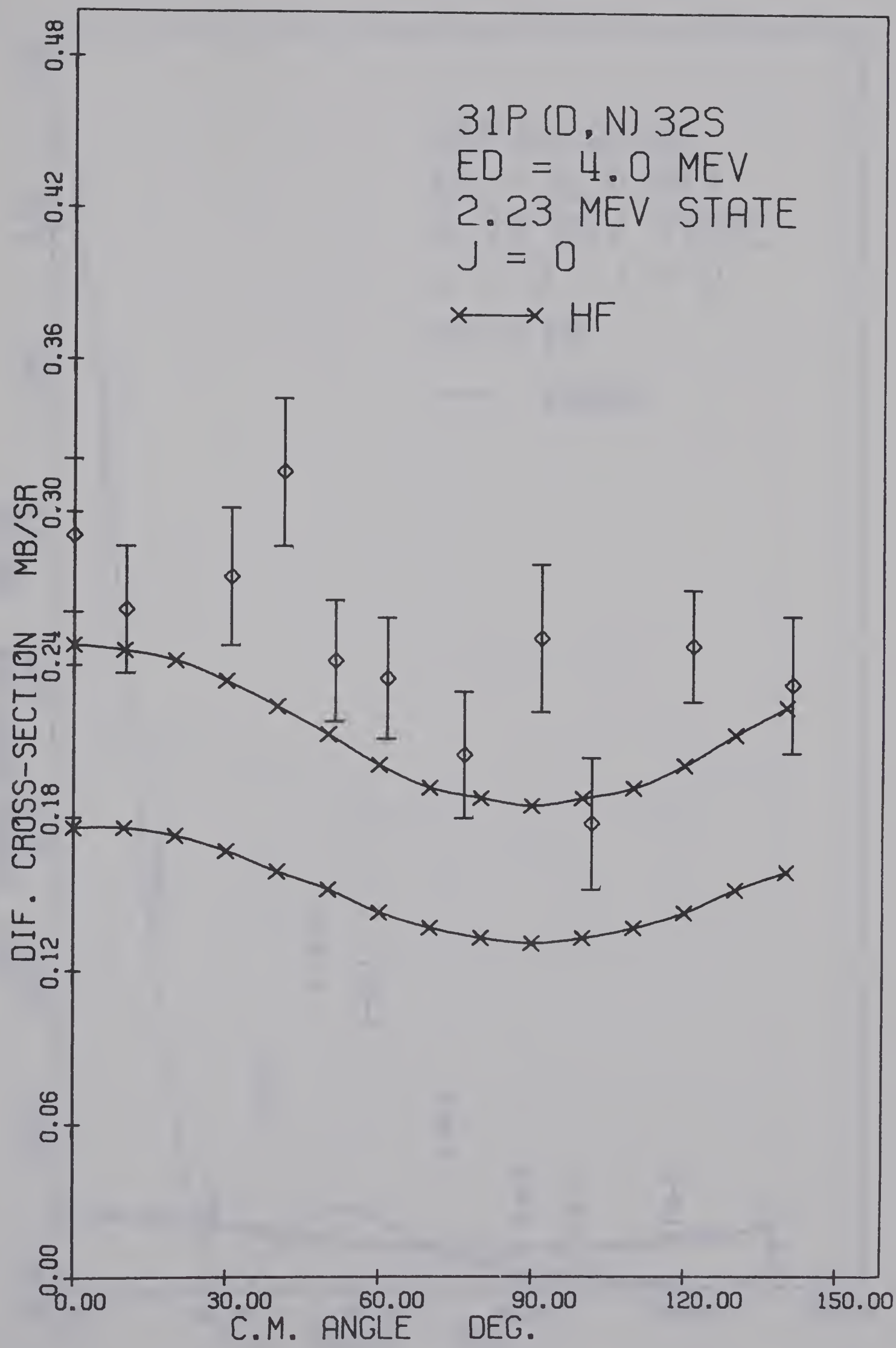
31P (D, N) 32S
ED = 4.0 MEV
2.23 MEV STATE
J = 0
HF
DIF. CROSS-SECTION MB/SR
0.00
0.06
0.12
0.18
0.24
0.30
0.36
0.42
0.48
0.00
30.00
60.00
90.00
120.00
150.00
C.M. ANGLE DEG.

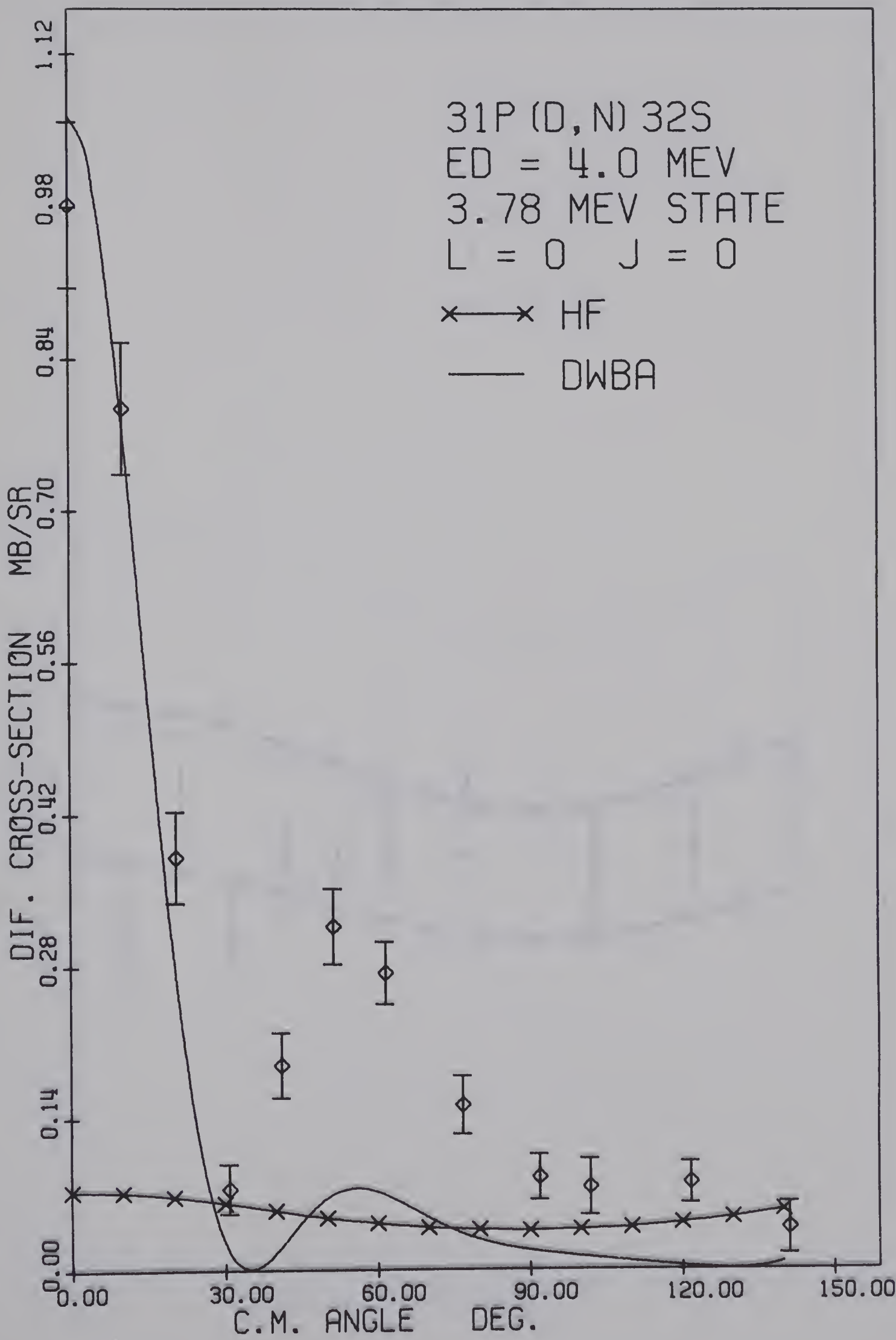
31P (D, N) 32S
ED = 4.0 MEV
3.78 MEV STATE
L = 0 J = 0
HF
DWBA
DIF. CROSS-SECTION MB/SR
0.00
0.14
0.28
0.42
0.56
0.70
0.84
0.98
1.12
0.00
30.00
60.00
90.00
120.00
150.00
C.M. ANGLE DEG.

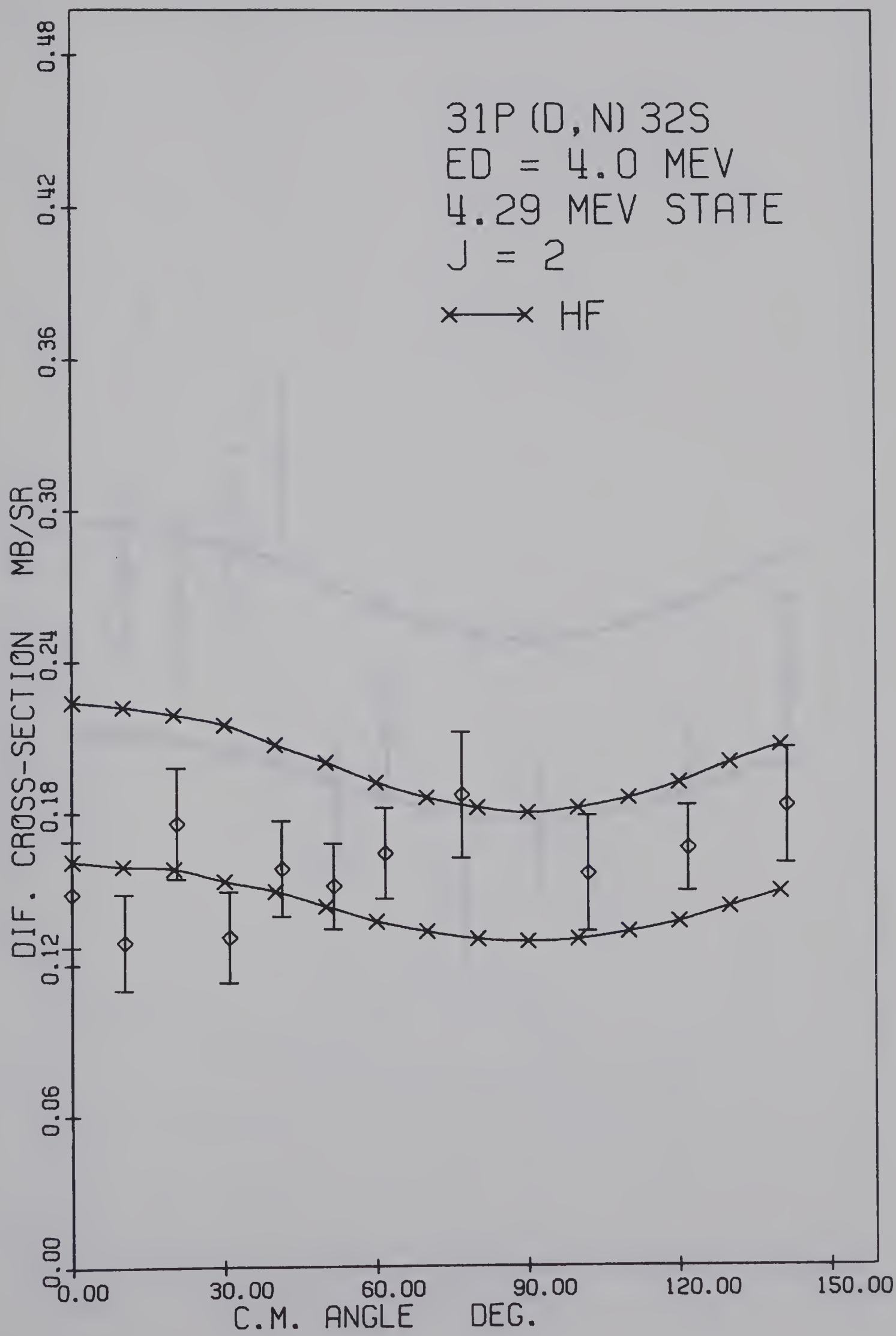
31P (D, N) 32S
ED = 4.0 MEV
4.29 MEV STATE
J = 2
HF
DIF. CROSS-SECTION MB/SR
0.00
0.06
0.12
0.18
0.24
0.30
0.36
0.42
0.48
0.00
30.00
60.00
90.00
120.00
150.00
C.M. ANGLE DEG.

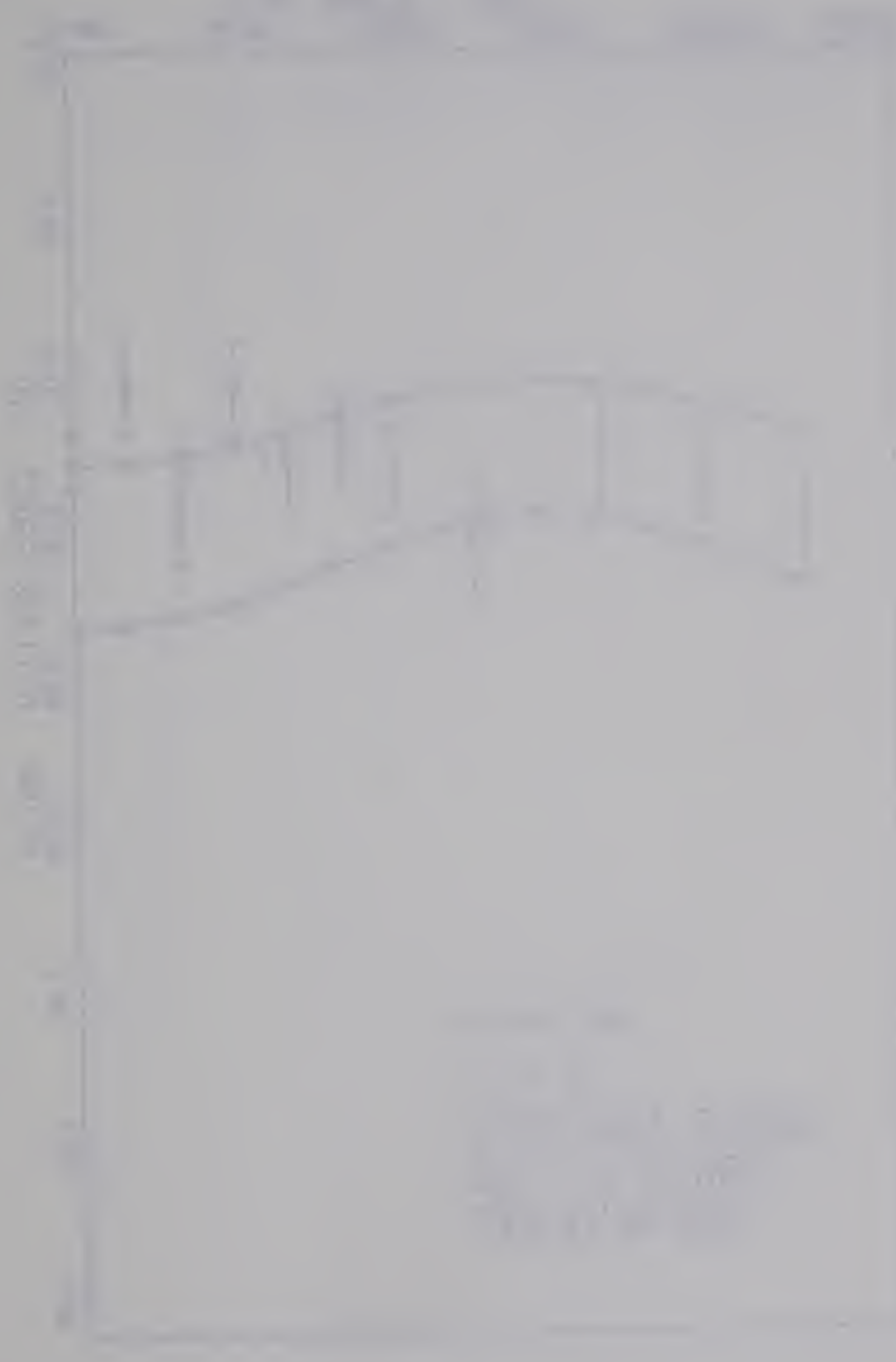

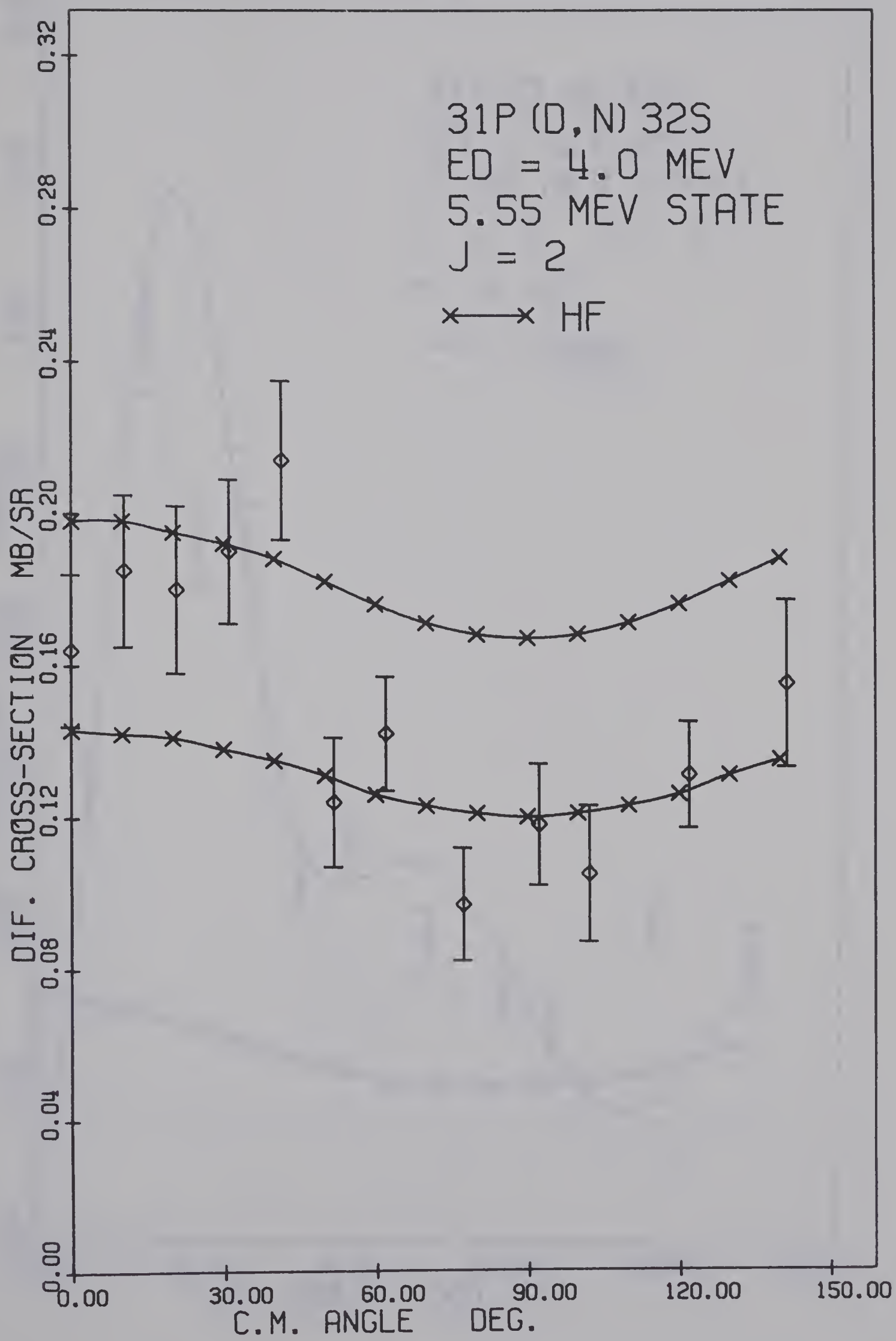
31P (D, N) 32S
ED = 4.0 MEV
5.55 MEV STATE
J = 2
HF
DIF. CROSS-SECTION MB/SR
0.00
0.04
0.08
0.12
0.16
0.20
0.24
0.28
0.32
0.00
30.00
60.00
90.00
120.00
150.00
C.M. ANGLE DEG.

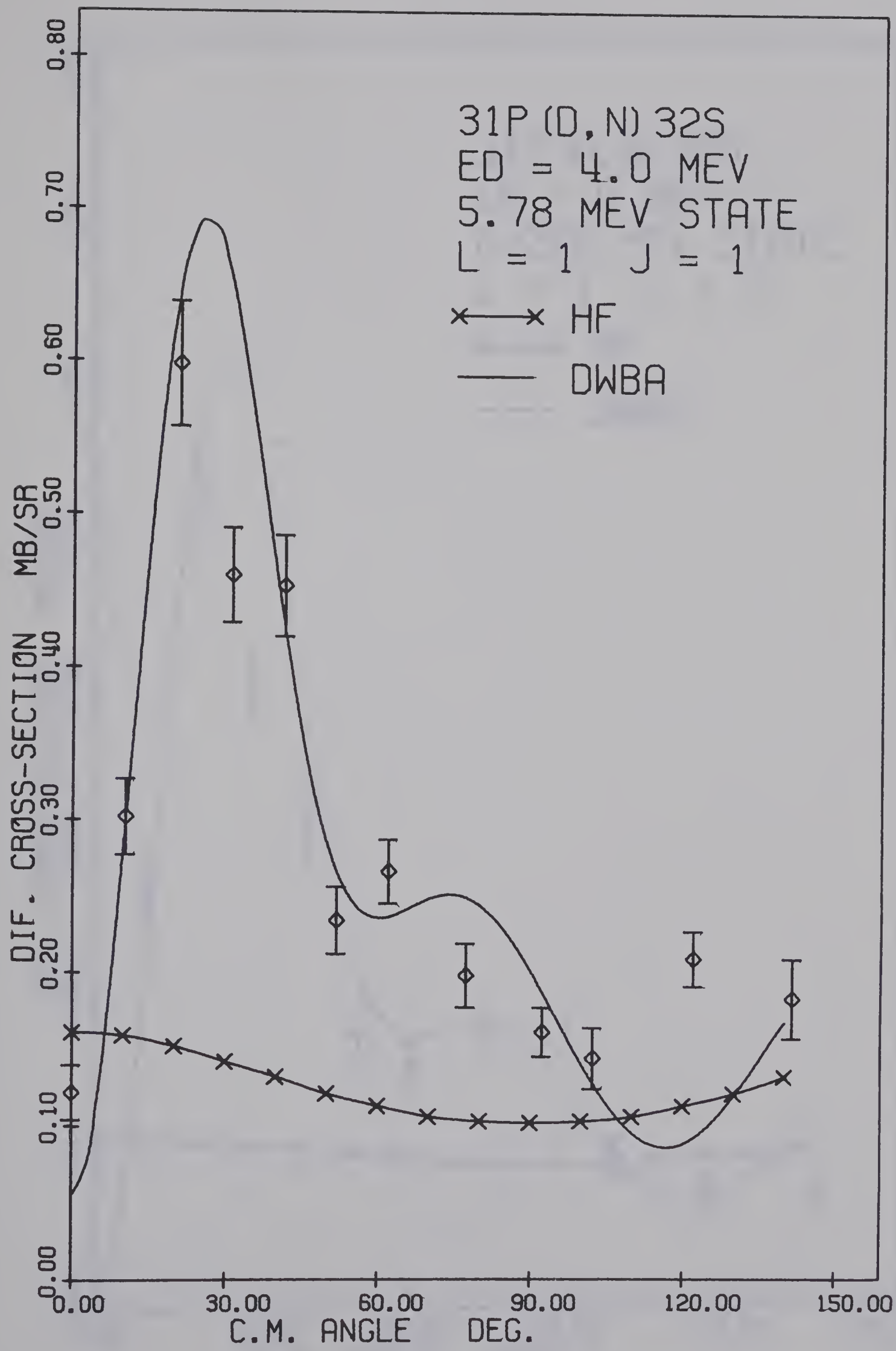
31P (D, N) 32S
ED = 4.0 MEV
5.78 MEV STATE
L = 1 J = 1
HF
DWBA
DIF. CROSS-SECTION MB/SR
0.00
0.10
0.20
0.30
0.40
0.50
0.60
0.70
0.80
0.00
30.00
60.00
90.00
120.00
150.00
C.M. ANGLE DEG.

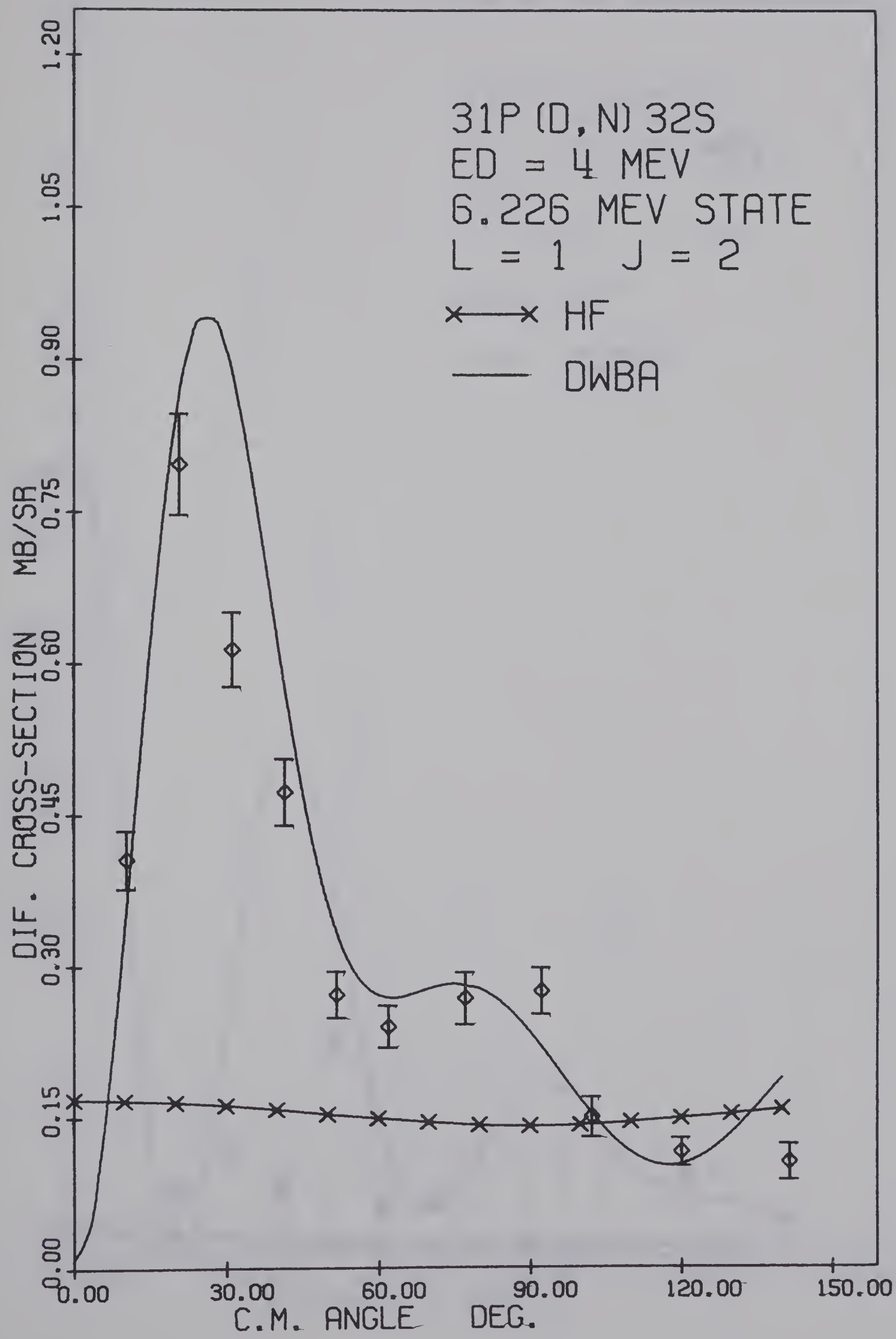
31P (D, N) 32S
ED = 4 MEV
6.226 MEV STATE
L = 1 J = 2
HF
DWBA
DIF. CROSS-SECTION MB/SR
0.00
0.15
0.30
0.45
0.60
0.75
0.90
1.05
1.20
0.00
30.00
60.00
90.00
120.00
150.00
C.M. ANGLE DEG.

DIF. CROSS-SECTION MB/SR

0.00 0.15 0.30 0.45 0.60 0.75 0.90 1.05 1.20

C.M. ANGLE DEG.

0.00 30.00 60.00 90.00 120.00 150.00

31P (D,NJ 32S
ED = 5.45 MEV
G.S.
L = 0 J = 0

HF

DWBA

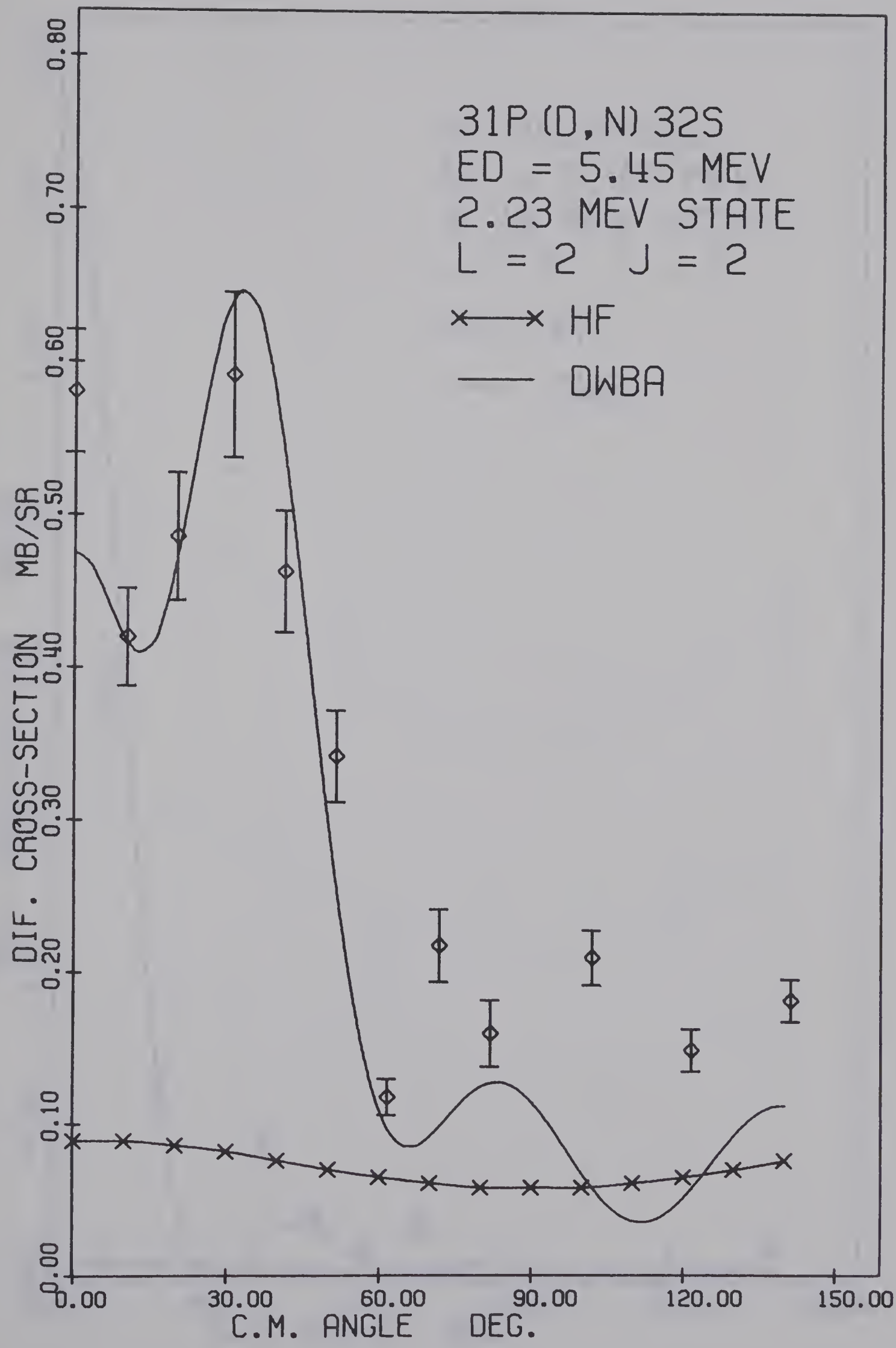
31P (D, N) 32S
ED = 5.45 MEV
2.23 MEV STATE
L = 2 J = 2
HF
DWBA
DIF. CROSS-SECTION MB/SR
0.00
0.10
0.20
0.30
0.40
0.50
0.60
0.70
0.80
0.00
30.00
60.00
90.00
120.00
150.00
C.M. ANGLE DEG.

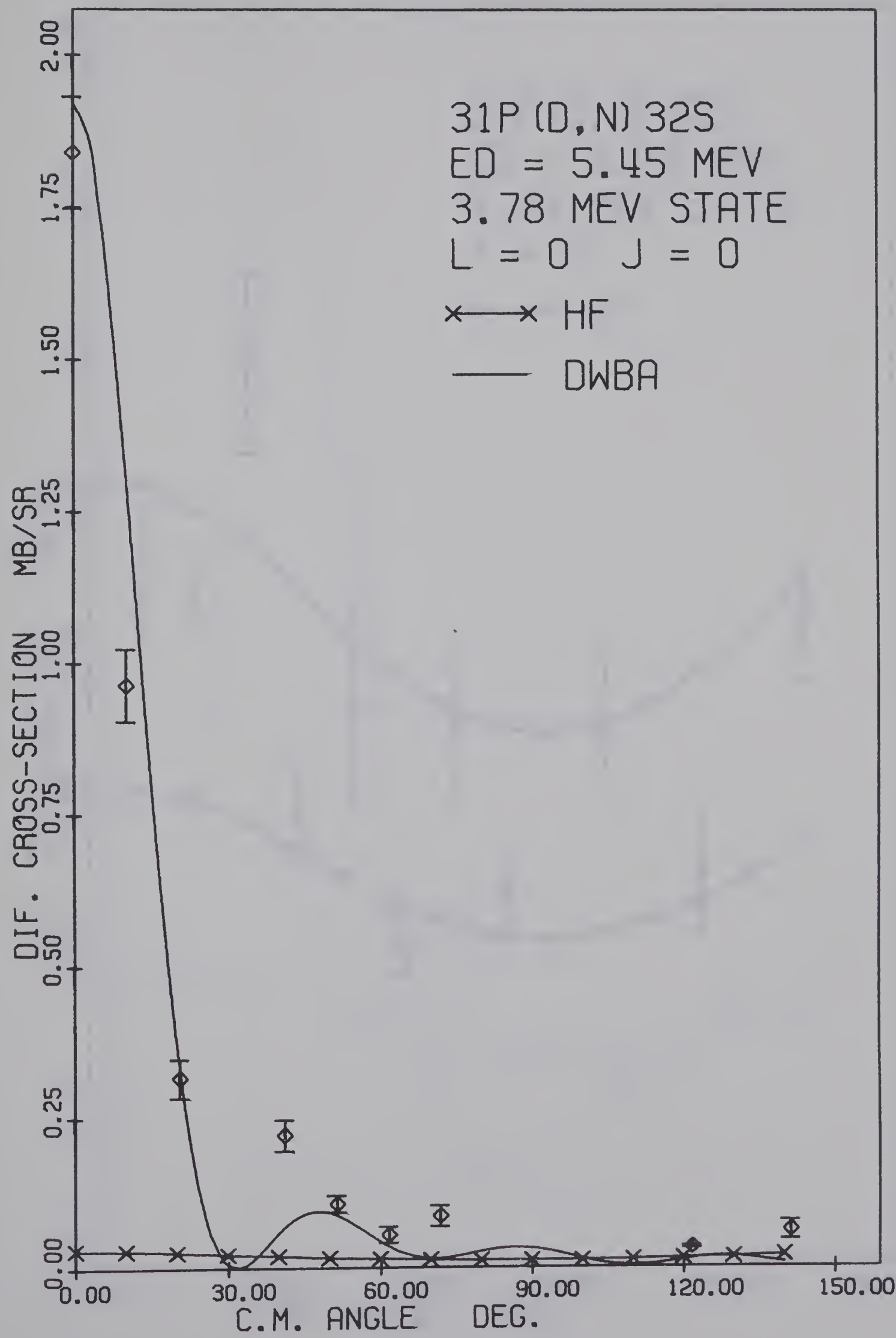
31P (D, N) 32S
ED = 5.45 MEV
3.78 MEV STATE
L = 0 J = 0
HF
DWBA
DIF. CROSS-SECTION MB/SR
0.00
0.25
0.50
0.75
1.00
1.25
1.50
1.75
2.00
0.00
30.00
60.00
90.00
120.00
150.00
C.M. ANGLE DEG.

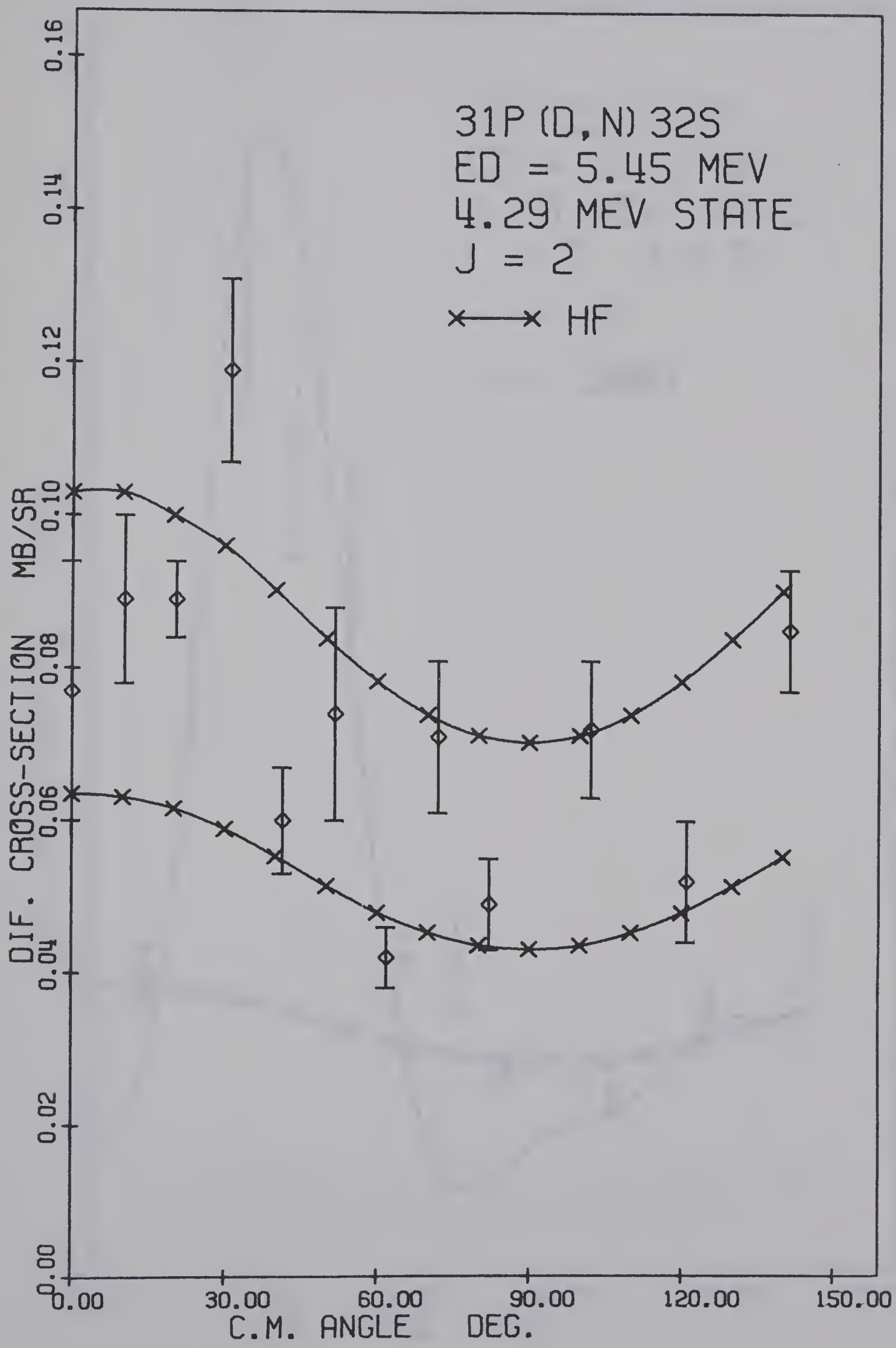
31P (D, N) 32S
ED = 5.45 MEV
4.29 MEV STATE
J = 2
HF
DIF. CROSS-SECTION MB/SR
0.00
0.02
0.04
0.06
0.08
0.10
0.12
0.14
0.16
0.00
30.00
60.00
90.00
120.00
150.00
C.M. ANGLE DEG.

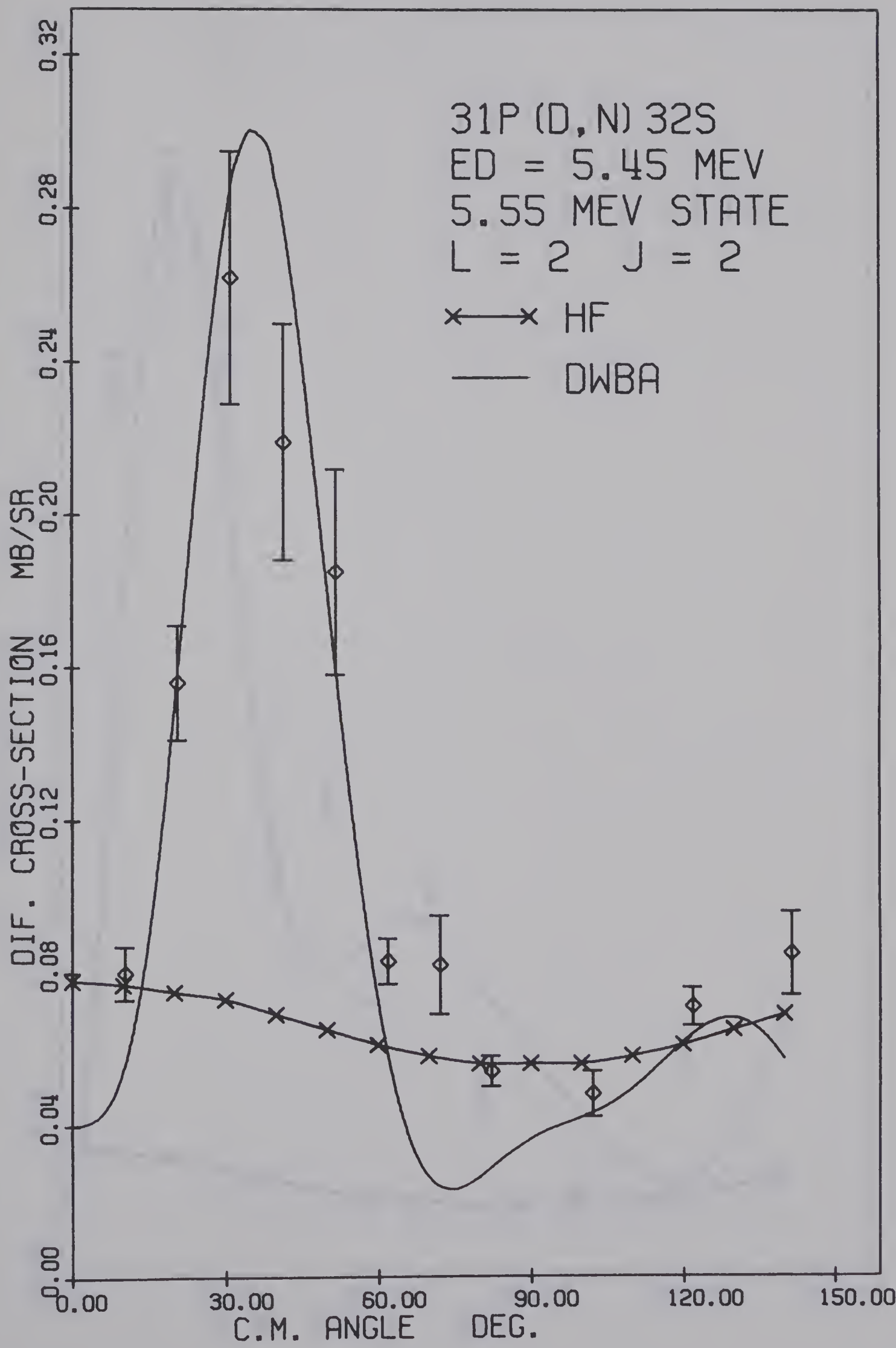
31P (D, N) 32S
ED = 5.45 MEV
5.55 MEV STATE
L = 2 J = 2
HF
DWBA
DIF. CROSS-SECTION MB/SR
0.00
0.04
0.08
0.12
0.16
0.20
0.24
0.28
0.32
0.00
30.00
60.00
90.00
120.00
150.00
C.M. ANGLE DEG.

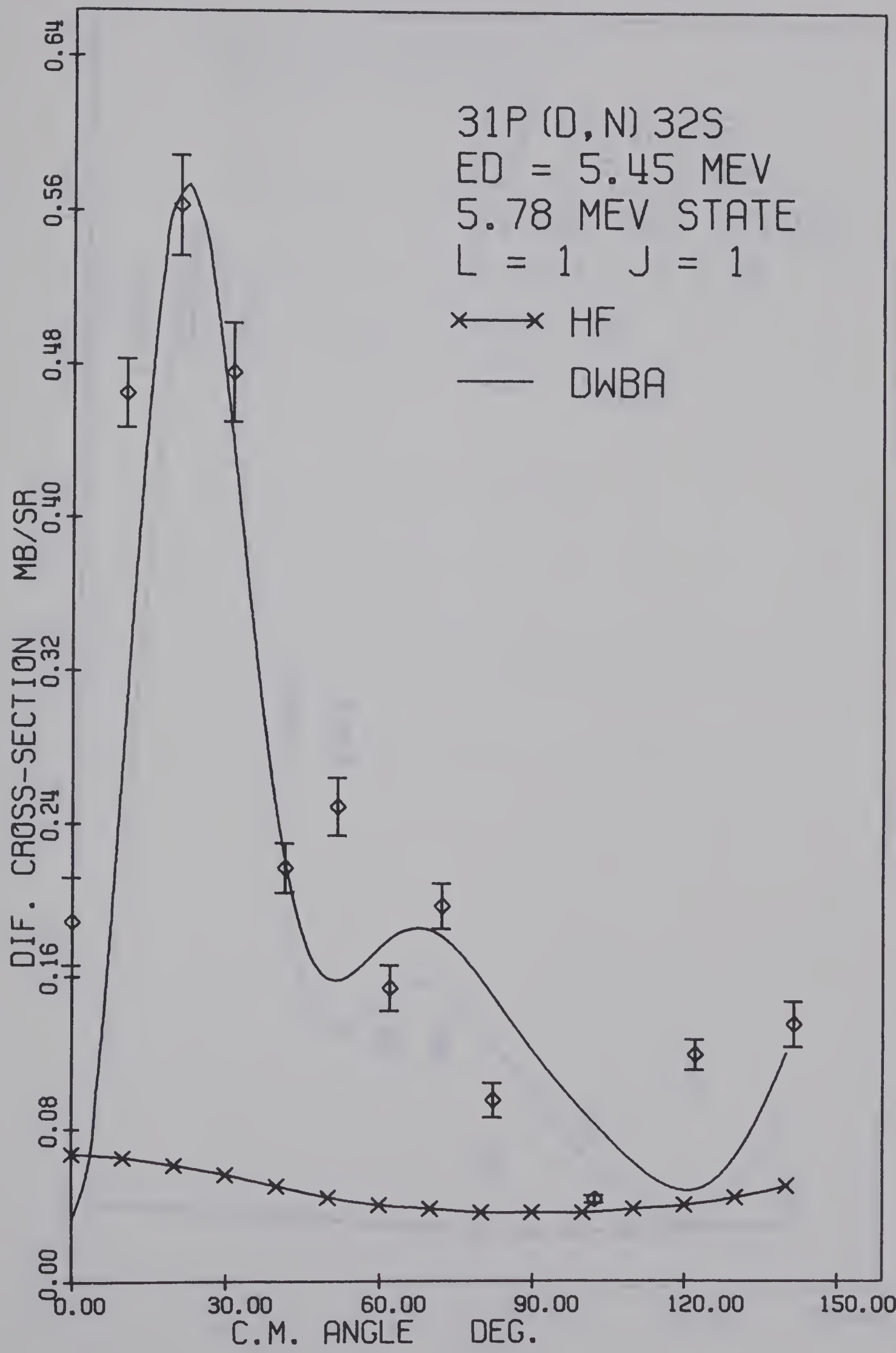
31P (D, N) 32S
ED = 5.45 MEV
5.78 MEV STATE
L = 1 J = 1
HF
DWBA
DIF. CROSS-SECTION MB/SR
0.00
0.08
0.16
0.24
0.32
0.40
0.48
0.56
0.64
0.00
30.00
60.00
90.00
120.00
150.00
C.M. ANGLE DEG.

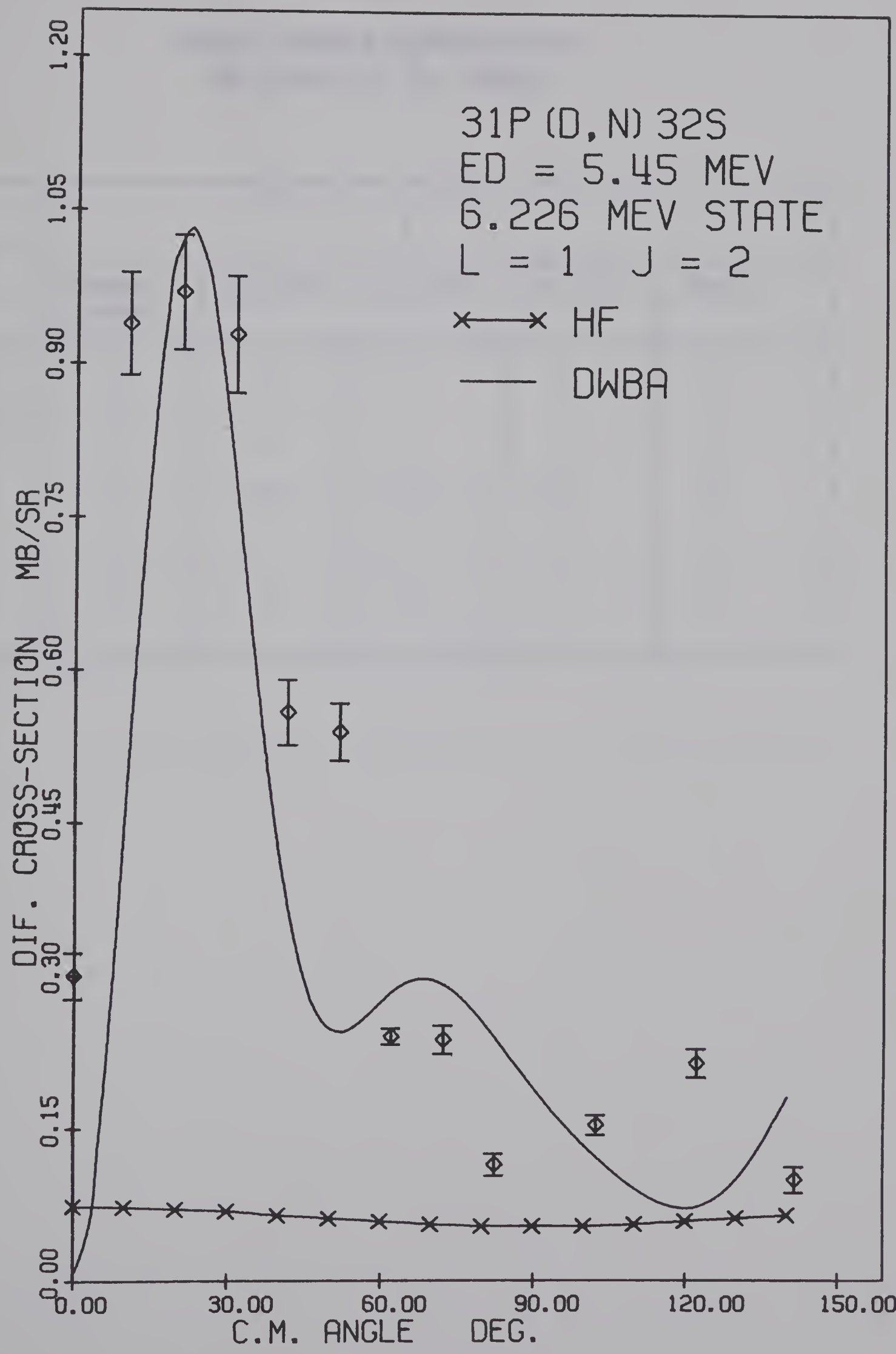
31P (D, N) 32S
ED = 5.45 MEV
6.226 MEV STATE
L = 1 J = 2
HF
DWBA
DIF. CROSS-SECTION MB/SR
0.00
0.15
0.30
0.45
0.60
0.75
0.90
1.05
1.20
0.00
30.00
60.00
90.00
120.00
150.00
C.M. ANGLE DEG.

TABLE 4-3

ANGULAR MOMENTUM TRANSFER VALUES
FOR LEVELS IN ^{32}S NUCLEUS

E_x MeV	ℓ_p				
	Present Work	(Fu 68)	(Gr 68)	(Mo 70)	(En 67)
G.S.	0	0	0	0	0
2.237	2	2	2	2	2
3.78	0	0	0	0	0
5.55	2	2	2	2	2
6.23	1	1	1	1	1

compound mechanisms),

$$\left(\frac{d\sigma}{d\Omega}\right)_{exp} = \left(\frac{d\sigma}{d\Omega}\right)_{comp} + \left(\frac{d\sigma}{d\Omega}\right)_{Dir}$$

$$\left(\frac{d\sigma}{d\Omega}\right)_{Dir} = C^2 S \left(\frac{d\sigma}{d\Omega}\right)_{DW}$$

where $\left(\frac{d\sigma}{d\Omega}\right)_{DW}$ is the differential cross-section given by DWUK code, S is the spectroscopic factor, and C is the isospin Clebsch-Gordan coefficient which is given by:

$$C = \langle T_p T_n T_{Zp} T_{Zn} | T_d T_{Zd} \rangle \langle T_X T_p T_{ZX} T_{Zp} | T_Y T_{ZY} \rangle$$

where T is the isospin, T_Z is the Z-component of T and subscripts, p,n,d,X and Y stands for proton, neutron, deuteron, target and residual nucleus respectively. In our case of $^{31}P(d,n)^{32}S$ $C = \frac{1}{2}$.

Table 4-4 compares our prediction for S and those given by (Gr 68), (Mo 70), and (Gl 64).

TABLE 4-4

THE SPECTROSCOPIC FACTORS FOR
^{32}S LEVELS UNDERSTUDY

		S				
		Present Work		Experimental		Theor.
E_x MeV	J^π	4.00 MeV	5.45 MeV	(Gr 68)	(Mo 70)	(G1 64)
G.S.	0^+	2.63	2.20	2.4	2.2	2.8
2.237	2^+		1.195	1.2	1.3	1.05
3.78	0^+	0.45	0.41	0.4	0.66	0.47
5.55	2^+		0.17	0.13	0.2	
5.78	1^-	0.15	0.11	0.19	0.26	
6.23	$(1,2)^-$	0.12*	0.11*	0.12*	0.19*	

* Calculated for $J^\pi = 2^-$

CHAPTER 5

DISCUSSIONS AND CONCLUSIONS

It is evident from Figs. 4-1 - 4-14 that DWBA fitting is quite good for all states that show a direct pattern. The only exception for this is the ground state, where the DWBA calculations show an unusually high second peak. This may be due to inadequate optical potential for the deuteron or the outgoing neutron. In spite of this inadequacy for the ground state the fitting for all other states is quite consistent at both deuteron energies.

Many optical model parameters, extracted from deuteron elastic scattering experiments on different neighboring nuclei and in the energy range of 4-15 MeV, have been tried for calculations. These trials show a large variations in the deduced spectroscopic factors. This fact stressed the need for "reliable" optical model parameters.

It is desirable to extract the optical model parameters from deuteron elastic scattering experiment on the same nucleus and at the same energy as those of the (d,n) experiment.

Table 4-4 show that there is a quite good agreement between the spectroscopic factors deduced from this work and those deduced from (He^3,d) work (Gr 68, and Mo 70) and the theoretical predictions of Glaudmans et al. (Gl 64). This agreement confirms the idea that ^{28}Si can be used as a core for describing the shell structure of ^{32}S .

The Glaudmans et al.(Gl 64) shell model calculations has been carried out for several states observed in ^{32}S . These calculations predict

the detailed wave-function and spectroscopic factors, by assuming a ^{28}Si core, and employing two-particle interaction between all possible configurations involving the extra-core 2S1/2 and 1d3/2 nucleons. Detailed wave functions of ^{31}P G.S. and ^{32}S G.S., 2.237 and 3.78 MeV states are displayed in table 5-1. Glaudmans notation has been used in this table. This notation can be explained as follows. The configuration $\underset{10\underline{31}}{S2d1}$ in $^{31}P(J = \frac{1}{2}, T = \frac{1}{2})$ ground state wave function refers to two 2S1/2 particles coupled to $J = 1$ and $T = 0$ and one 1d3/2 particle with $J = 3/2$ and $T = 1/2$, so underlining indicates half-integers. The two terms are then coupled to the final $J = 1/2$ and $T = 1/2$. The numerical entries are intensities intenths of a percent for the various pure wave functions at the top of each column. The sign refers to phases.

TABLE 5-1

Shell-Model Wave-Functions Used to Calculate
The Theoretical Spectroscopic Factors

	S3 11	S2d1 1031	S1d2 1101	S1d2 1110	d3 11
$^{31}P(1/2,1/2)\ E_x = 0.0$	-675	4	-288	-27	7

	S4 00	S2d2 0101	S2d2 1010	S1d3 1111	d4 00
$^{32}S(0,0)\ E_x = 0.0$	-496	391	59	-12	-42
$^{32}S(0,0)\ E_x = 3.78$	468	242	92	-12	-186

	S3d1 1131	S2d2 1030	S2d2 1010	S2d2 0121	S1d3 1131
$^{32}S(2,0)\ E_x = 2.237$	-689	7	-5	28	-240

	S1d3 1151	d4 20	d4 20"
$^{32}S(2,0)\ E_x = 2.237$	8	20	-3

APPENDIX A

TABLES OF DIFFERENTIAL CROSS-SECTIONS

TABLE A-1

DIFFERENTIAL CROSS-SECTION FOR
THE GROUND STATE

E_d = 4.00 MeV			E_d = 5.45 MeV		
θ° C.M.	$(d\sigma/d\Omega)_{C.M.}$ mb/sr	Error mb/sr	θ° C.M.	$(d\sigma/d\Omega)_{C.M.}$ mb/sr	Error mb/sr
0.0	0.351	0.043	0.0	0.836	0.046
10.27	0.270	0.030	10.30	0.402	0.029
20.54	0.079	0.019	20.59	0.067	0.009
30.79	0.152	0.020	30.86	0.096	0.010
41.01	0.180	0.027	41.11	0.070	0.009
51.21	0.126	0.025	51.32	0.209	0.013
61.36	0.109	0.019	61.50	0.052	0.007
91.57	0.090	0.021	71.62	0.057	0.008
101.55	0.085	0.031	121.50	0.081	0.007
121.36	0.091	0.018	141.11	0.041	0.005
141.01	0.090	0.026			

TABLE A-2

DIFFERENTIAL CROSS-SECTION FOR
THE 2.23 MeV-STATE

E_d = 4.0 MeV			E_d = 5.45 MeV		
θ° C.M.	$(d\sigma/d\Omega)_{C.M.}$ mb/sr	Error mb/sr	θ° C.M.	$(d\sigma/d\Omega)_{C.M.}$ mb/sr	Error mb/sr
0.0	0.291	0.030	0.0	0.581	0.040
10.31	0.262	0.025	10.33	0.420	0.032
20.61	0.433	0.035	20.66	0.486	0.042
30.89	0.275	0.027	30.96	0.592	0.054
41.14	0.316	0.029	41.23	0.463	0.040
51.36	0.242	0.024	51.47	0.342	0.030
61.54	0.235	0.024	61.66	0.118	0.012
76.71	0.205	0.025	71.80	0.218	0.024
91.77	0.251	0.029	81.89	0.160	0.022
101.75	0.178	0.026	101.89	0.210	0.018
121.54	0.248	0.22	121.60	0.149	0.014
141.14	0.233	0.027	141.23	0.182	0.014

TABLE A-3

DIFFERENTIAL CROSS-SECTION FOR
THE 3.78 MeV-STATE

E_d = 4.0 MeV			E_d = 5.45 MeV		
θ° C.M.	$(d\sigma/d\Omega)_{C.M.}$ mb/sr	Error mb/sr	θ° C.M.	$(d\sigma/d\Omega)_{C.M.}$ mb/sr	Error mb/sr
0.0	0.982	0.076	0.0	1.840	0.092
10.34	0.795	0.061	10.36	0.964	0.060
20.67	0.381	0.042	20.72	0.316	0.032
30.98	0.075	0.023	41.34	0.221	0.026
41.26	0.189	0.030	51.60	0.107	0.014
51.51	0.317	0.035	61.81	0.055	0.014
61.70	0.274	0.029	71.97	0.086	0.018
76.90	0.152	0.027	121.81	0.033	0.002
91.97	0.085	0.021	141.35	0.061	0.016
101.94	0.076	0.026			
121.70	0.080	0.019			
141.26	0.038	0.024			

TABLE A-4

DIFFERENTIAL CROSS-SECTION FOR
4.28 MeV-STATE

E_d = 4.0 MeV			E_d = 5.45 MeV		
θ° C.M.	$(d\sigma/d\Omega)_{C.M.}$ mb/sr	Error mb/sr	θ° C.M.	$(d\sigma/d\Omega)_{C.M.}$ mb/sr	Error mb/sr
0.0	0.148	0.021	0.0	0.077	0.017
10.36	0.129	0.019	10.38	0.089	0.011
20.70	0.176	0.022	20.74	0.089	0.005
31.02	0.131	0.018	31.08	0.119	0.012
41.32	0.158	0.019	41.39	0.060	0.007
51.57	0.151	0.017	51.66	0.074	0.014
61.77	0.164	0.018	61.87	0.042	0.004
76.98	0.187	0.025	72.03	0.071	0.010
92.05	0.268	0.026	82.13	0.049	0.006
102.02	0.156	0.023	102.13	0.072	0.009
121.77	0.166	0.017	121.03	0.052	0.008
141.32	0.183	0.023	141.39	0.085	0.008

TABLE A-5

DIFFERENTIAL CROSS-SECTION FOR
5.55 MeV-STATE

	E_d = 4.0 MeV		E_d = 5.45 MeV		
θ° C.M.	$(d\sigma/d\Omega)_{C.M.}$ mb/sr	Error mb/sr	θ° C.M.	$(d\sigma/d\Omega)_{C.M.}$ mb/sr	Error mb/sr
0.0	0.164	0.020	10.41	0.080	0.007
10.40	0.185	0.020	20.81	0.156	0.015
20.79	0.180	0.022	31.19	0.262	0.033
31.15	0.190	0.019	41.52	0.219	0.031
41.48	0.214	0.021	51.82	0.185	0.027
51.76	0.124	0.017	62.05	0.083	0.006
61.99	0.142	0.015	72.23	0.082	0.013
77.22	0.097	0.015	82.33	0.054	0.004
92.30	0.118	0.016	102.33	0.048	0.005
102.26	0.105	0.018	122.05	0.071	0.005
121.99	0.131	0.014	141.52	0.085	0.011
141.48	0.155	0.022			

TABLE A-6

DIFFERENTIAL CROSS-SECTION FOR
5.78 MeV

E_d = 4.0 MeV			E_d = 5.45 MeV		
θ° C.M.	$(d\sigma/d\Omega)_{C.M.}$ mb/sr	Error mb/sr	θ° C.M.	$(d\sigma/d\Omega)_{C.M.}$ mb/sr	Error mb/sr
0.0	0.122	0.018	0.0	0.189	0.023
10.41	0.302	0.025	10.42	0.465	0.018
20.81	0.598	0.041	20.83	0.563	0.026
31.18	0.460	0.031	31.21	0.476	0.026
41.51	0.453	0.033	41.55	0.217	0.013
51.81	0.234	0.022	51.85	0.249	0.015
62.04	0.266	0.021	62.09	0.154	0.012
77.28	0.198	0.021	72.27	0.197	0.012
92.36	0.161	0.016	82.38	0.095	0.009
102.32	0.144	0.020	102.38	0.043	0.002
122.04	0.209	0.018	122.09	0.119	0.008
141.51	0.183	0.026	141.55	0.135	0.012

TABLE A-7

DIFFERENTIAL CROSS-SECTION FOR
6.226 MeV-STATE

E_d = 4.0 MeV			E_d = 5.45 MeV		
θ° C.M.	$(d\sigma/d\Omega)_{C.M.}$ mb/sr	Error mb/sr	θ° C.M.	$(d\sigma/d\Omega)_{C.M.}$ mb/sr	Error mb/sr
10.41	0.406	0.029	0.0	0.300	0.023
20.81	0.797	0.050	10.44	0.939	0.050
31.18	0.614	0.037	20.86	0.970	0.056
41.51	0.473	0.033	31.25	0.929	0.057
51.81	0.272	0.023	41.61	0.559	0.032
62.04	0.240	0.021	51.92	0.540	0.028
77.28	0.268	0.026	62.17	0.241	0.008
92.36	0.275	0.023	72.36	0.238	0.014
102.32	0.150	0.020	82.47	0.115	0.011
120.04	0.115	0.014	102.47	0.154	0.010
141.51	0.105	0.018	122.17	0.215	0.014
			141.61	0.100	0.013

REFERENCES

Au 53 N. Austern, Phys. Rev. 89 (1953) 318.

Ba 61 A.M. Baldin, V.I. Goldaskii and R.I. Rosensal, Kinematics of Nuclear Reactions, Translated from Russian by W.E. Jones, (Pergamon Press, 1961).

Bh 52 A.B. Bhatia, K. Huang, R. Huby and C. Newns, Phil. Mag. 43 (1952) 485.

Bl 52 J. Blatt and V.F. Wiesskopf, Theoretical Nuclear Physics, (John Wiley & Sons Inc., 1952).

Bo 70 J.J.W. Bogaards, Ph.D. Thesis, University of Alberta (1970).

Bu 51 S.T. Butler, Proc. Roy. Soc. A208 (1951) 559.

Bu 57 S.T. Butler and O.H. Hittmair, Nuclear Stripping Reactions (John Wiley & Sons, Inc., New York, 1957).

Ca 55 J.M. Calvert, A.A. Jaffe, A.E. Litherland and E.E. Maslin, Proc. Phys. Soc. A68 (1955) 1008.

Ch 61 R.L. Chase, Nuclear Pulse Spectroscopy (McGraw-Hill Book Company Inc., Toronto, 1961).

Da 68 N.E. Davison, University of Alberta Internal Report (1968).

Da 69 N.E. Davison, University of Alberta Internal Report UAE-NPL-7 (1969).

El 55 F.A. El Bedewi and M.A. Elwahab, Proc. Phys. Soc. A68 (1955) 754.

El 69 B. Elbek and P.O. Tjøm, Advances in Nuclear Physics, 3 (1969) 259.

En 67 P.M. Endt and C.Van der Leun, Nuclear Physics A105 (1967) 1.

Fe 68 A.T.G. Ferguson, L. Nilsson and N. Starfelt, Nuclear Physics A111 (1968) 423.

Fu 53 Y. Fujimoto, Proceedings of the International Conference of Theoretical Physics (Universities of Koyoto and Tokyo 1953).

Ge 67 D.A. Gedcke and W.J. McDonald, Nucl. Inst. & Meth. 55 (1967) 377.

Ge 67a D.A. Gedcke and W.J. McDonald, Nucl. Inst. & Meth. 56 (1967) 148.

Gl 63 N.K. Glendening, Ann. Rev. Nucl. Sci. 13 (1963) 191.

Gl 64 P.W.M. Glaudmans, G. Wiechers and P.J. Brussaard, Nuclear Physics 56 (1964) 548.

Gr 67 T.B. Grandy, Ph.D. Thesis, University of Alberta (1967).

Gr 68 A. Graue, L. Herland and J.R. Lien, Nuclear Physics A120 (1968) 513.

Gu 68 D.P. Gurd, G. Roy and, H.G. Leighton, Nuclear Physics A120 (1968) 94.

Ho 67 P.E. Hodgson, Ann. Rev. Nucl. Sci., 17 (1967) 1.

Ku 67 P.D. Kunz, University of Colorado, Private Communication (1967).

La 35 E.O. Lawrence, E. McMillan and L.R. Thoronton, Phys. Rev. 48 (1935) 493.

La 58 A.M. Lane and R.G. Thomas, Rev. Mod. Phys. 30 (1958) 257.

Le 64 L.L. Lee, J.P. Schiffer, B. Zeidman, G.R. Satchler, R.M. Drisko and R.M. Bassel, Phys. Rev. 136 (1964) B971.

Mo 70 R.A. Morrison, Nuclear Physics A140 (1970) 97.

Ne 56 T.D. Newton, Can. J. Phys. 34 (1956) 804.

Ne 59 G.C. Neilson, W.K. Dawson and F.A. Johnson, Rev. Sci. Inst. 30 (1959) 963.

Op 35 J.R. Oppenheimer and M. Phillips, Phys. Rev. 48 (1935) 500.

Ro 61 M.E. Rose, Elementary Theory of Angular Momentum (John Wiley & Sons Inc., 1961).

Sa 63 G.R. Satchler, Nuclear Physics 55 (1963) 1.

Sa 65 G.R. Satchler, Lectures in Theoretical Physics Vol. VIII C (University of Colorado Press 1965).

SM 65 W.R. Smith, Oak Ridge National Laboratory Internal Report ORNL-TM-1117 (1965).

Sm 65a W.R. Smith, Oak Ridge National Laboratory Internal Report ORNL-TM-1234 (1965).

Sm 68 D.L. Smith, R.G. Polk and T.G. Miller, Nucl. Inst. & Meth. 64 (1968) 157.

Te 66 W.J. Tepel, Nucl. Inst. & Meth. 40 (1966) 100.

To 54 W. Tobocman, Phys. Rev. 95 (1954) 1655.

To 61 W. Tobocman, Theory of Direct Nuclear Reactions (Oxford University Press, London, 1961).

Vo 68 E. Vogt, Advances in Nuclear Physics 1 (1968) 261.

Wi 63 D. Willmore and D.E. Hodgson, Nuclear Physics 55 (1963) 673.